

Likelihood Based Inference in Fully and Partially Observed Exponential Family Graphical Models with Intractable Normalizing Constants

Yujie Chen, Anindya Bhadra and Antik Chakraborty*

Department of Statistics, Purdue University

Abstract

Probabilistic graphical models that encode an underlying Markov random field are fundamental building blocks of *generative modeling* to learn *latent representations* in modern multivariate data sets with complex dependency structures. Among these, the exponential family graphical models are especially popular, given their fairly well-understood statistical properties and computational scalability to high-dimensional data based on pseudo-likelihood methods. These models have been successfully applied in many fields, such as the Ising model in statistical physics and count graphical models in genomics. Another strand of models allows some nodes to be *latent*, so as to allow the marginal distribution of the observable nodes to depart from exponential family to capture more complex dependence. These approaches form the basis of generative models in artificial intelligence, such as the Boltzmann machines and their restricted versions. A fundamental barrier to likelihood-based (i.e., both maximum likelihood and fully Bayesian) inference in both fully and partially observed cases is the intractability of the likelihood. The usual workaround is via adopting pseudo-likelihood based approaches, following the pioneering work of Besag (1974). The goal of this paper is to demonstrate that full likelihood based analysis of these models is feasible in a computationally efficient manner. The chief innovation lies in using a technique of Geyer (1991) to estimate the intractable normalizing constant, as well as its gradient, for intractable graphical models. Extensive numerical results, supporting theory and comparisons with pseudo-likelihood based approaches demonstrate the applicability of the proposed method.

Keywords: Boltzmann Machines, Contrastive Divergence, Generative models, Ising Model, Poisson Graphical Model.

*Correspondence: 150 N. University St., West Lafayette, IN 47907, USA. Email: antik015@purdue.edu.

1 Introduction

Exponential family graphical models provide a coherent framework for describing dependence in multivariate data. However, likelihood-based statistical inference is typically hindered by the presence of an intractable normalizing constant, and due to the lack of scalability of doubly intractable procedures (e.g., Murray et al., 2012; Møller et al., 2006; Liang, 2010), existing methods rely on pseudo-likelihood or approximate Bayesian methods to facilitate estimation (Ravikumar et al., 2010; Besag, 1974). Although these methods could be consistent under certain assumptions, it is a classical result that full likelihood methods are *statistically efficient*, at least in an asymptotic sense and for correctly specified models (Fisher, 1922; Rao, 1945). This apparent bottleneck also applies to the *partially observed exponential family graphical models*, where latent variables are introduced in such a way that the joint distribution of latent and observed variables belongs to an exponential family, although the marginal distribution of the observed variables may not. This leads to the so called *product of experts* family of models for the observed variables (Hinton et al., 1998; Hinton, 2002), which allows complicated dependence structure not belonging in the exponential family to be modeled, and is considered a foundational building block for *generative artificial intelligence*, through an architecture known as the *Hopfield Network* or *Boltzmann Machine* (Hopfield, 1982), whose purpose is to model Hebbian learning in the brain neural circuitry (Hebb, 1949). The intractable normalizing constant in this case has precluded a practically successful deployment of a full Boltzmann Machine so far, and has led to *reduced form architectures* where training is possible. For example, in Restricted Boltzmann Machines (RBM) or Deep Boltzmann Machines (DBM) (Hinton, 2007; Fischer and Igel, 2012; Salakhutdinov and Hinton, 2009), where observed multivariate data is modeled as the marginal distribution over unobserved hidden variables; a key assumption is the independence of the hidden variables given the visible variables, and vice versa, which leads to training by *approximate likelihood* based methods, such as the contrastive divergence (CD)

algorithm of [Hinton \(2002\)](#). Yet, it is known that with high probability the CD solution differs from the maximum likelihood solution ([Sutskever and Tieleman, 2010](#)), and the justification for the artificial bipartite grouping of latent and observed variables in an RBM, or its deep extensions such as the DBM ([Salakhutdinov and Hinton, 2009](#)), is primarily computational, rather than substantive.

To address these issues, this article develops an array of computationally feasible methods that enable full-likelihood based analysis (both maximum likelihood and fully Bayesian) for both fully and partially observed exponential family graphical models. This is achieved without resorting to computationally expensive *doubly intractable* Metropolis-Hastings approaches ([Murray et al., 2012](#); [Møller et al., 2006](#)), which allows our method to scale to hundreds of variables in both fully and partially observed cases. We also propose a technique, which we believe to be the first viable method, for training a *full* Boltzmann machine, without any restrictions on its architecture, such as a bipartite graph. The key to our scalability is sampling under the *independence model*, underlying any exponential family graphical model, which accomplishes two things. First, it allows us to use vanilla Monte Carlo instead of running a prohibitive MCMC scheme after each parameter update as in CD. Second, we show that the variance of the importance sampling estimate is well controlled with our choice. We also develop theoretical results for likelihood based inference in both fully and partially observed cases. These have received little attention so far, due to the computational intractability of likelihood-based inference, in the first place.

The remainder of this article is organized as follows. In [Section 2](#) we provide the necessary background material on fully and partially observed exponential family graphical models, where for the latter we focus in particular on Boltzmann machines and their variants. The main methodological innovation is discussed in [Section 3](#), where we outline the use of [Geyer \(1991\)](#) for computing the intractable likelihood and its gradient. Applications to fully and partially observed models are discussed in [Section 4](#) and [5](#), followed by the-

oretical properties of likelihood-based inference in Section 6. Numerical experiments and data analysis results are in 7 and 8, followed by concluding remarks in Section 9.

2 Preliminaries

2.1 Pairwise *fully observed* exponential family graphical models

Consider a graph $G = (V, E)$ with $|V| = p$ nodes. Associate each node with a random variable X_j with sample space \mathcal{X}_j , for $j = 1, \dots, p$. The edge set consists of pairs (j, k) such that the nodes j and k are connected. We assume the connection is undirected, i.e. if $(j, k) \in E$ then $(k, j) \in E$. A clique $C \subset V$ of a graph is a fully-connected subset of vertices. Define \mathcal{C} to be the set of all cliques of the graph. A probability distribution on the graph can be defined using a product of clique-wise compatibility functions ψ_C , i.e.,

$$p(x_1, \dots, x_p) = \frac{1}{z} \prod_{C \in \mathcal{C}} \psi_C(x_C), \quad (1)$$

where z is such that $p(x_1, \dots, x_p)$ is a valid density or mass function. Valid distributions such as (1) under certain conditions can be arrived at from another perspective. Indeed, consider the node-conditional distribution $X_j | X_{-j}$, i.e. the conditional distribution of X_j given the other variables. Suppose this distribution belongs to the univariate exponential family of models. Then, by the Hammersley–Clifford theorem (Lauritzen, 1996), the joint distribution produced by these node-conditional distribution is of the form (1). This particular class of models is known as exponential family graphical models (Yang et al., 2015), for which the compatibility functions for each clique are the dot product of the respective sufficient statistics and the parameter of the distribution. When the clique set is the set of all nodes and the set of all edges, one obtains what is known as the pairwise exponential

family graphical models (PEGM), with pdf given by:

$$p_{\theta}(x_1, \dots, x_p) = \frac{1}{z(\theta)} \exp \left\{ \sum_{j \in V} \theta_j T_j(x_j) + \sum_{(j,k) \in E} \theta_{jk} T_{jk}(x_j, x_k) + \sum_{j \in V} C(x_j) \right\}, \quad (2)$$

where $T_j(x_j)$ and $T_{jk}(x_j, x_k)$ are the sufficient statistics, and $\theta \in \Theta \subset \mathbb{R}^{p \times p}$ is the parameter matrix with $\theta_{jk} = \theta_j$ if $j = k$ and $\theta_{jk} = \theta_{kj}$ if $j \neq k$. Further generalizations of these models when the cliques are not restricted to be the set of vertices and edges are discussed in [Yang et al. \(2015\)](#). Conditional independence structures in (2) can also be defined in terms of the pairwise parameters θ_{jk} , since $\theta_{jk} = 0$ if and only if $(j, k) \notin E$. In other words, $X_j \perp\!\!\!\perp X_k \mid X_{-(j,k)}$ if and only if $\theta_{jk} = 0$. It is straightforward to observe that if X has density given by (2), then the node-conditional distribution of $X_j \mid X_{-j}$ is:

$$p_{\theta}(x_j \mid x_{-j}) = \frac{1}{z(\theta; x_{-j})} \exp \left\{ \theta_j T_j(x_j) + C(x_j) + 2 \sum_{k \in N(j)} \theta_{jk} T_{jk}(x_j, x_k) \right\},$$

where $z(\theta; x_{-j})$ is the normalizing constant belonging to a univariate exponential family distribution for $(X_j \mid X_{-j})$, and $N(j)$ denotes all neighbors of j , as encoded by G . The parameter space Θ for which (2) is a valid probability model is convex ([Barndorff-Nielsen, 1978](#); [Wainwright and Jordan, 2008](#)) and the sample space is $\mathcal{X} = \mathcal{X}_1 \times \dots \times \mathcal{X}_p$. When Θ is open, the model is said to be regular. Some specific PEGM examples are as follows.

Example 2.1. (*Ising*). The Ising model ([Ising, 1924](#)) is a PEGM with $C(x_j) = 0$, $T_j(x_j) = x_j$ and $T_{jk}(x_j, x_k) = x_j x_k$. Moreover, $X_j \mid X_{-j}$ has a Bernoulli distribution with natural parameter $\theta_j + 2 \sum_{k \in N(j)} \theta_{jk} x_k$. The sample space for this model is $\{0, 1\}^p$ and $\Theta = \mathbb{R}^{p \times p}$.

Example 2.2. (*PGM*). The Poisson graphical model (PGM), proposed by [Besag \(1974\)](#), and further developed by [Yang et al. \(2013\)](#) is a PEGM with $C(x_j) = \log x_j!$, $T_j(x_j) = x_j$ and $T_{jk}(x_j, x_k) = x_j x_k$. Here $X_j \mid X_{-j} \sim \text{Poi}(\theta_j + 2 \sum_{k \in N(j)} \theta_{jk} x_k)$. The sample space is $\{\mathbb{N} \cup \{0\}\}^p$, i.e. the set of all p -dimensional count vectors, and Θ is the set of all $p \times p$ real matrices with non-positive off-diagonal elements.

Other examples include the Potts model (Potts, 1952), or the truncated Poisson graphical model (Yang et al., 2013). In all of the examples above, likelihood-based inference is generally infeasible due to the intractability of $z(\theta)$ and available methods approximate the likelihood $\ell(\theta)$ by $\prod_j \ell(X_j | X_{-j})$, the *pseudo-likelihood*. There are two key reasons for this: (1) $X_j | X_{-j}$ is a member of a univariate exponential family and (2) due to the product form of the pseudo-likelihood, inference can be carried out in parallel for the p nodes.

2.2 Pairwise *partially observed* exponential family graphical models: product of experts and *approximate* maximum likelihood via contrastive divergence

Consider a binary vector $\mathbf{v} \in \{0, 1\}^p$ which might encode the on and off pixels of a black-and-white image. In generative artificial intelligence (AI), the goal is to learn the underlying features of the distribution of \mathbf{v} so that high-quality synthetic data from the trained AI can be produced for new content. One potential modeling choice could be an exponential family model, e.g., the Ising. For modern complex data such as images, this restriction to exponential family could severely limit the model’s ability to capture more complex dependence not belonging to the exponential family. As an alternative, Boltzmann Machines have emerged as one of the fundamental tools for generative AI. These can be thought of as stochastic neural networks represented by a graph that encodes symmetric connections between observed variables and hidden or latent variables (Ackley et al., 1985). The joint distribution of the p observed and m hidden variables are assumed to belong to a PEGM (Ising in this case): $p_\theta(\mathbf{v}, \mathbf{h}) = z(\theta)^{-1} \exp(-E_\theta(\mathbf{v}, \mathbf{h}))$ where $E_\theta(\mathbf{v}, \mathbf{h})$ is known as the energy function in the literature and $z(\theta) = \sum_{\mathbf{v}, \mathbf{h}} \exp(-E_\theta(\mathbf{v}, \mathbf{h}))$. Specifically,

$$\log p_\theta(\mathbf{v}, \mathbf{h}) = \sum_j \theta_{jj} v_j + \sum_k \theta_{kk} h_k + \sum_{j \neq j'} \theta_{jj'} v_j v_{j'} + \sum_{k \neq k'} \theta_{kk'} h_k h_{k'} + \sum_{j,k} \theta_{jk} v_j h_k - \log z(\theta),$$

for $j, j' = 1, \dots, p$; $k, k' = p+1, \dots, p+m$ and $\theta \in \mathbb{R}^{(p+m) \times (p+m)}$. The marginal distribution of the visible variables, $p_\theta(\mathbf{v}) = \sum_{\mathbf{h}} p_\theta(\mathbf{v}, \mathbf{h})$, does not necessarily belong to the exponential family. Introduction of the hidden variables allows one to describe complex dependency structures in the visible variables using simple conditional distributions. Moreover, the hidden variables act as non-linear feature detectors (Hinton, 2007). It can be seen that for this model, the gradient of the log-likelihood for a visible sample \mathbf{v} is:

$$\frac{\partial \ell(\theta)}{\partial \theta} = \frac{\partial \log \sum_{\mathbf{h}} p_\theta(\mathbf{v}, \mathbf{h})}{\partial \theta} = \sum_{v,h} \frac{\partial E_\theta(\mathbf{v}, \mathbf{h})}{\partial \theta} p_\theta(\mathbf{v}, \mathbf{h}) - \sum_{v,h} \frac{\partial E_\theta(\mathbf{v}, \mathbf{h})}{\partial \theta} p_\theta(\mathbf{h} | \mathbf{v}), \quad (3)$$

where (3) can be interpreted as the difference of two expectations: expected value of the gradient of the energy function under the joint distribution of (\mathbf{v}, \mathbf{h}) and under the conditional distribution of $\mathbf{h} | \mathbf{v}$. For most general versions of this model, existing learning algorithms approximate either both or at least one of these two terms using MCMC sampling, which is too slow for practical deployment, and lacks scalability to larger dimensions.

Equation (3) also illustrates that the most general version of the Boltzmann machine is hard to train and computationally demanding, which has paved the way for simplified versions of Boltzmann machines, specifically the restricted Boltzmann machine (RBM) where the underlying graph is bipartite. RBM (Smolensky, 1986) is inspired by the biological connectivity network among neurons. RBM's multi-layer extension, or deep Boltzmann machine (DBM) (Salakhutdinov et al., 2007) has proven to be a popular machine learning tool for unsupervised learning (Zhang et al., 2019) and is a *universal approximator* for any distribution over $\{0, 1\}^p$ (Le Roux and Bengio, 2008; Montufar and Ay, 2011). Adjacent layers of a DBM have the same architecture as an RBM. Figure 1 shows the graphical model for a BM, RBM and a DBM with three hidden layers.

Learning in the RBM is facilitated by the conditional independence of the hidden variables given the visible variables and vice versa. Specifically, for RBM: $-E_\theta(\mathbf{v}, \mathbf{h}) = \sum_k \theta_{kk} h_k + \sum_j \theta_{jj} v_j + \sum_j \sum_k \theta_{jk} v_j h_k$, which implies $\mathbb{P}(h_k = 1 | \mathbf{v}) = \sigma(\theta_{kk} + \sum_j \theta_{jk} v_j)$ and

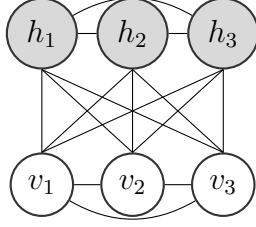


Fig. 1(a): BM

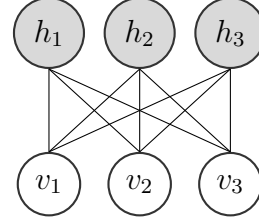


Fig. 1.(b): RBM

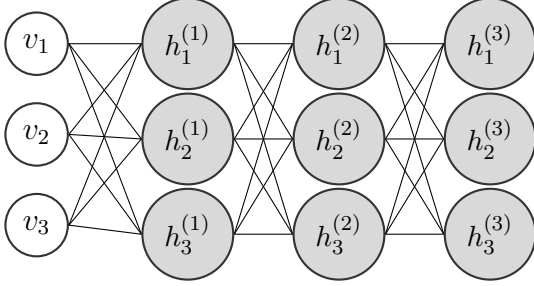


Fig. 1.(c): DBM

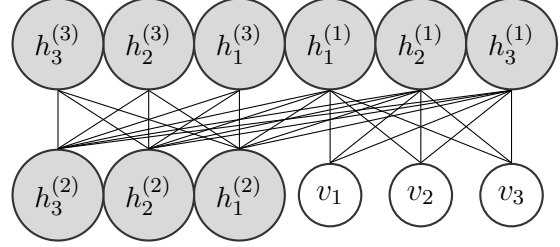


Fig. 1.(d): DBM rearranged as an RBM

Figure 1: From left to right: BM, RBM, DBM with three visible nodes. DBM has three layers of hidden variables. The notation is: hidden nodes ($h_j \in \{0, 1\}$, shaded in gray), visible nodes ($v_k \in \{0, 1\}$, transparent). Deep hidden nodes in layer l are denoted by $h^{(l)}$.

$\mathbb{P}(v_j = 1 \mid \mathbf{h}) = \sigma(\theta_{jj} + \sum_k \theta_{jk} h_k)$ where $\sigma(x) = \{1 + \exp(-x)\}^{-1}$, $x \in \mathbb{R}$ is the logistic sigmoid function. The bipartite dependence structure gives a *product of experts* marginal model for the visible variables (Fischer and Igel, 2012):

$$p_{\theta}(\mathbf{v}) = z(\theta)^{-1} \prod_{j=1}^p \exp(\theta_{jj} v_j) \prod_{k=p+1}^{p+m} \left(1 + \exp(\theta_{kk} + \sum_{j=1}^p \theta_{jk} v_j) \right). \quad (4)$$

The contrastive divergence (CD) algorithm (Hinton, 2002) is an approximate procedure for finding the MLE under this model via gradient ascent. Suppose $\theta = \theta^{(t)}$ at iteration t . Using (3) for an RBM one obtains:

$$\nabla_{\theta^{(t)}} \log p_{\theta_t}(\mathbf{h}, \mathbf{v}) = \langle \mathbf{h}\mathbf{v}^T \rangle_{\text{data}} - \langle \mathbf{h}\mathbf{v}^T \rangle_{\text{model}},$$

where the angle brackets with subscript “data” denote an expectation with respect to $p_{\theta^{(t)}}(\mathbf{h} \mid \mathbf{v})$ at the observed \mathbf{v} , which is analytic; and those with subscript “model” denote an expectation with respect to $p_{\theta^{(t)}}(\mathbf{h}, \mathbf{v})$; which is typically not available in closed form and

is evaluated using MCMC. However, the difficulty here is that direct and exact simulation from $p_{\theta^{(t)}}(\mathbf{h}, \mathbf{v})$ is infeasible. Thus, the CD algorithm uses a Gibbs sampler to iteratively sample $(\mathbf{h} \mid \mathbf{v}, \theta^{(t)})$ and $(\mathbf{v} \mid \mathbf{h}, \theta^{(t)})$. The key issues are:

1. The procedure requires running a new Gibbs sampler every time $\theta^{(t)}$ is updated, until convergence to the target distribution $p_{\theta^{(t)}}(\mathbf{h}, \mathbf{v})$ is achieved. This is reminiscent of the double MH procedure (Liang, 2010), which is computationally prohibitive and is one of the primary motivations behind the bipartite graph of RBM that allows *batch sampling* of $\mathbf{h} \mid \mathbf{v}, \theta^{(t)}$ and $\mathbf{v} \mid \mathbf{h}, \theta^{(t)}$ by drawing independent Bernoulli vectors. The conditional independence structure is lost if one allows within layer connections, precluding the use of more general Boltzmann machines.
2. Even for an RBM with batch sampling, convergence to the stationary target $p_{\theta^{(t)}}(\mathbf{h}, \mathbf{v})$ is only achieved if the chain is run for $K \rightarrow \infty$ MCMC iterations at every iteration t , under standard MCMC theory. In practice, the CD algorithm is only run for a small K (CD- K) or even $K = 1$ Gibbs iterations for every t . In this case, it can be shown that CD is not an estimate of the gradient of *any* function (Section 4, Sutskever and Tieleman, 2010). Thus, gradient ascent cannot converge to the MLE, although in practice it might have reasonable practical performance.

3 A Monte Carlo estimate of $z(\theta)$ and its Gradient for Exponential Family Graphical Models

Let $p_{\theta}(x) = q_{\theta}(x)/z(\theta)$, $x \in \mathbb{R}^p$ be a probability density function such that $z(\theta) = \int q_{\theta}(x)dx = \exp(A(\theta))$ and $\theta \in \Theta$. Consider the situation where the explicit form of $q_{\theta}(x)$ is known for any θ in the parameter space and is computationally cheap to evaluate but the analytical form of $z(\theta)$ is intractable for every $\theta \in \Theta$. Given n independent observations from such a model, form the matrix $\mathbf{X} \in \mathbb{R}^{n \times p}$. For notational convenience, we

later use $\mathbf{X} = (X_1, \dots, X_p)$, where each X_j is understood to be a vector of the j th variable over n samples for $j = \{1, \dots, p\}$. Otherwise, when the indexing is over the i th row of \mathbf{X} , it is made explicit by writing $X_{i\bullet}$ for $i = \{1, \dots, n\}$. Let the log-likelihood at two parameter values $\theta, \phi \in \Theta$ be $\ell(\theta)$ and $\ell(\phi)$, respectively. Then,

$$\ell(\theta) - \ell(\phi) = \log \frac{p_\theta(\mathbf{X})}{p_\phi(\mathbf{X})} = \sum_{i=1}^n \log \frac{q_\theta(X_{i\bullet})}{q_\phi(X_{i\bullet})} - n \log \frac{z(\theta)}{z(\phi)},$$

where the ratio $z(\theta)/z(\phi)$ cannot be explicitly computed. However, [Geyer \(1991\)](#) noted:

$$\frac{z(\theta)}{z(\phi)} = \frac{1}{z(\phi)} \int q_\theta(x) dx = \frac{1}{z(\phi)} \int \frac{q_\theta(x)}{q_\phi(x)} q_\phi(x) dx = \int \frac{q_\theta(x)}{q_\phi(x)} p_\phi(x) dx = \mathbb{E}_{Y \sim p_\phi} \left[\frac{q_\theta(Y)}{q_\phi(Y)} \right], \quad (5)$$

motivating the Monte Carlo estimate $\frac{1}{N} \sum_{i=1}^N \frac{q_\theta(Y_{i\bullet})}{q_\phi(Y_{i\bullet})}$, where $Y_{i\bullet} \stackrel{i.i.d.}{\sim} p_\phi$. For any generic $\phi \in \Theta$, the node-conditional distributions can be used to devise a Markov chain Monte Carlo (MCMC) scheme to sample from p_ϕ . However, if specific choices of ϕ are available such that independent samples are possible to simulate cheaply, then these samples could also be utilized to approximate the expectation. Moreover, if for such a ϕ , the corresponding normalizing constant $z(\phi)$ is available in closed form, one has an estimate of $z(\theta)$, for all θ . The key to the current work is our choice: $\boxed{\phi = \text{diag}(\theta)}$. With this choice: (a) a sample $Y \sim p_\phi$ can be obtained by sampling $Y_j \sim p_{\theta_{jj}}$ independently and setting $Y = (Y_1, \dots, Y_p)$, and (b) $z(\phi)$ is analytically tractable. This is in general true for any PEGM since the independent model is simply a distribution over p -univariate exponential families, and a few examples are provided next. For the Ising model, $z(\phi) = \prod_{j=1}^p z(\theta_{jj}) = \prod_{j=1}^p (1 + \exp(\theta_{jj}))$. For the Poisson Graphical model, $z(\phi) = \prod_{j=1}^p z(\theta_{jj}) = \prod_{j=1}^p \exp(\exp(\theta_{jj}))$. For observed samples \mathbf{X} , the log-likelihood is $\ell(\theta) = \sum_{i=1}^n \log q_\theta(X_{i\bullet}) - n \log z(\theta)$. To obtain the maximum likelihood estimator of θ , one can use the gradient ascent method leading to updates of the form $\theta^{(t+1)} = \theta^{(t)} + \gamma \nabla_\theta \ell(\theta) = \theta^{(t)} + \gamma [\sum_{i=1}^n \nabla_\theta \log q_\theta(X_{i\bullet}) - n \nabla_\theta \log z(\theta)]$, where γ is a suitable step-size. Clearly, for such an algorithm to succeed, one needs access

to the gradient $\nabla_{\theta} \log z(\theta) = \nabla_{\theta} z(\theta)/z(\theta)$. In the next proposition, an unbiased estimate for $\nabla_{\theta} z(\theta)$ is proposed, similar in spirit to the estimate of $z(\theta)$.

Proposition 3.1.

$$\frac{\nabla_{\theta} z(\theta)}{z(\phi)} = \mathbb{E}_{Y \sim p_{\phi}} \left[\frac{\nabla_{\theta} q_{\theta}(Y)}{q_{\phi}(Y)} \right].$$

Proof. In (5) replace $z(\theta)$ with $\nabla_{\theta} z(\theta)$ and differentiate under the integral sign. \square

While the Monte Carlo version of estimates of $z(\theta)$ and $\nabla_{\theta} z(\theta)$ are unbiased by construction, their practical utility is determined by their variance, which need not be bounded for an arbitrary ϕ (Geyer and Thompson, 1992). However, for our specific choice of ϕ , the following key proposition establishes that the variances of Monte Carlo estimates of $z(\theta)$ and $\nabla_{\theta} z(\theta)$ are finite under mild conditions.

Proposition 3.2. *Let $u = \theta - \text{diag}(\theta)$, and $\phi = \text{diag}(\theta)$. Then, (a) Monte Carlo estimate for $z(\theta)$ has bounded variance if $(2u + \phi) \in \Theta$ and, moreover, (b) the Monte Carlo estimate of $\nabla_{\theta} z(\theta)$ also has bounded variance if $(2(1 + \delta)u + \phi) \in \Theta$ for some $\delta > 0$.*

Refer to Supplementary Section S.1.1 for a proof of Proposition 3.2. We proceed to make several remarks on the implications of this proposition.

Remark 3.1. *Note that, $\frac{1}{1+\delta}(2(1 + \delta)u + \phi) + \frac{\delta}{1+\delta}\phi = 2u + \phi$. Thus, by the convexity of exponential family parameter space (see, e.g., Theorem 9.1 of Barndorff-Nielsen, 1978), the result of Proposition 3.2, Part (b) implies that of Part (a), for all $\delta > 0$.*

Remark 3.2. *Note that if $\phi = \phi_0$ is an arbitrary reference point not depending on θ , the Monte Carlo variance of the importance ratio $q_{\theta}(X)/q_{\phi_0}(X)$ can easily become unbounded, even if $\phi_0 \in \Theta$. This is observed, for example, in a Poisson graphical model, by choosing a ϕ_0 , such that $\text{offdiag}(\theta - \phi_0) > 0$. This shows the importance of setting $\phi = \text{diag}(\theta)$, and the technique of Geyer (1991) is not very useful under an arbitrary ϕ , possibly explaining why the technique has not been widely attempted in this model. Setting $\phi = \text{diag}(\theta)$ removes*

the first order $T_j(X_j)$ terms from the ratio $q_\theta(X)/q_\phi(X)$, which is helpful for bounding the variance of what remains.

Remark 3.3. Another benefit of setting $\phi = \text{diag}(\theta)$, is that one is (exactly) sampling from the independence model $p_\phi(\cdot)$ for the purpose of Monte Carlo, which allows batch sampling, and is computationally far more efficient than (approximately) sampling from $p_\theta(\cdot)$ at every iteration, for which an iterative technique such as MCMC must be deployed. Variations of this latter approach, i.e., sampling auxiliary data Y_1, \dots, Y_N under $p_\theta(\cdot)$ given the current θ to approximate $z(\theta)$ and $\nabla_\theta \log z(\theta)$, are used in the double Metropolis–Hastings of [Liang \(2010\)](#), the contrastive divergence approach of [Hinton \(2002\)](#) that is popular for fitting a restricted Boltzmann machine ([Salakhutdinov et al., 2007](#)), and the Hamiltonian Monte Carlo approach under intractable likelihood as in [Stoehr et al. \(2019\)](#). All of these are based on the identity $\nabla_\theta \log z(\theta) = \mathbb{E}_{Y \sim p_\theta} \{\nabla_\theta(\log q_\theta(Y))\}$, for which the RHS can be approximated by $N^{-1} \sum_{i=1}^N \nabla_\theta(\log q_\theta(Y_{i\bullet}))$, where $Y_{1\bullet}, \dots, Y_{N\bullet} \stackrel{i.i.d.}{\sim} p_\theta$. The need to sample iteratively from $p_\theta(\cdot)$ lies at the heart of the lack of scalability for MCMC based methods, in both fully Bayesian as well as approximate maximum likelihood calculations for doubly intractable models. The choice of $\phi = \text{diag}(\theta)$, and subsequent sampling from p_ϕ , eliminates this difficulty, resulting in far greater scalability.

Remark 3.4. Although not our main focus, the same construction may potentially be used to design a simple MCMC-free sampler for $p_\theta(\cdot)$. See [Supplementary Section S.2](#) for details.

The following result provides further support on the well-behaved nature of our Monte Carlo estimates, providing exponential concentration bounds.

Proposition 3.3. Consider the class of PEGMs in (2) with $T_j(x_j) = x_j$ and $T_{jk}(x_j, x_k) = x_j x_k$ and suppose the j th sample space is bounded in the interval $[a_j, b_j]$ for $j = 1, \dots, p$. Set $U = q_\theta(Y)/q_\phi(Y)$ and $V = \nabla_{\theta_{jk}} q_\theta(Y)/q_\phi(Y)$ with $Y \sim p_\phi$. Then for every θ , both U and V as a function of Y have bounded differences in the sense of [Boucheron et al. \(2003\)](#),

Corollary 1). Moreover, there exists $C > 0$ such that for every $t > 0$, $\mathbb{P}[|U - \mathbb{E}(U)| > t] \leq 2 \exp\{-t^2/4C\}$, and $\mathbb{P}[|V - \mathbb{E}(V)| > t] \leq 2 \exp\{-t^2/4C\}$.

The proof is given in Supplementary Section S.1.2. Proposition 3.3 establishes that for PEGMs with finite support, the specific choice of $\phi = \text{diag}(\theta)$ not only leads to finite variance Monte Carlo estimates of $z(\theta)$ and $\nabla_{\theta} z(\theta)$, but for this specific class, the estimates are sub-Gaussian, which, in turn, implies exponential concentration of the sample mean of U, V . The class of PEGMs with finite support is quite rich. Indeed, the Ising model, Potts model, and the truncated Poisson graphical model are all members of this family.

4 Applications to Fully Observed Intractable Pairwise Exponential Family Graphical Models

4.1 MLE and Bayesian inference in low dimensions

Suppose we observe i.i.d. data $\mathbf{X} = (X_{1\bullet}, \dots, X_{n\bullet})$ where $X_{i\bullet}$'s are observations from a PEGM with density $p_{\theta}(x) = q_{\theta}(x)/z(\theta)$. The maximum likelihood estimate satisfies $\hat{\theta} = \arg \max_{\theta \in \Theta} \ell(\theta)$ or $\nabla_{\theta} \ell(\hat{\theta}) = 0$ where $\ell(\theta) = \sum_{i=1}^n \log q_{\theta}(X_{i\bullet}) - \log z(\theta)$. Denote $\log q_{\theta}(\mathbf{X}) = \sum_{i=1}^n \log q_{\theta}(X_{i\bullet})$. The estimate can be obtained by implementing a gradient ascent algorithm subject to the constraint $\theta \in \Theta$. We achieve this by the method of projected gradient ascent, which is a special case of proximal methods under box type constraints such as ours (p. 149, Parikh and Boyd, 2014). The projection operation is defined as $\mathcal{P}_{\Theta}(\theta^*) = \arg \min_{\theta \in \Theta} \|\theta - \theta^*\|_2^2$. Thus, the updates of the gradient ascent algorithm have the form:

$$\theta^{(t+1)} = \mathcal{P}_{\Theta}(\tilde{\theta}^{(t+1)}) = \mathcal{P}_{\Theta} \left(\theta^{(t)} + \gamma \nabla_{\theta} \ell(\theta^{(t)}) \right) = \mathcal{P}_{\Theta} \left(\theta^{(t)} + \gamma \frac{\nabla_{\theta} q_{\theta^{(t)}}(\mathbf{X})}{q_{\theta^{(t)}}(\mathbf{X})} - \gamma \frac{\nabla_{\theta} z(\theta^{(t)})}{z(\theta^{(t)})} \right), \quad (6)$$

where $\gamma > 0$ is the step size. For the Ising model, $\Theta = \mathbb{R}^{p \times p}$, hence \mathcal{P}_Θ is simply the identity map. However, for the Poisson graphical model, $\Theta = \{\theta : \theta_{jj} \in \mathbb{R}, \theta_{jk} \leq 0, j \neq k = 1, \dots, p\}$, for which \mathcal{P}_Θ simply amounts to thresholding any positive $\{\tilde{\theta}^{(t+1)}\}_{jk, j \neq k}$, computed via the gradient ascent step, to zero.

For Bayesian inference, consider proper priors $\pi(\theta)$ such that $\int_\Theta \pi(d\theta) = 1$ and assume $\nabla_\theta \pi(\theta)$ exists. Then, $U(\theta) = -\log \pi(\theta | \mathbf{X}) = -\ell(\theta) - \log \pi(\theta) + \log m(\mathbf{X})$ where $m(\mathbf{X}) = \int_\Theta \ell(\theta) \pi(\theta) d\theta$. Posterior sampling is usually achieved by constructing a random walk Markov kernel that transitions from the current state θ to a new candidate state θ' . Existing algorithms for doing this (Liang, 2010; Møller et al., 2006; Murray et al., 2012) are based on generating auxiliary samples from the candidate θ' . However, it is well known that the Hamiltonian Monte Carlo sampler could be more efficient in exploring a complicated likelihood surface compared to random walk Metropolis kernels, since the former uses gradient information for the MCMC updates (Neal et al., 2011). This often leads to better exploration of the target density, and the advantages could be substantial in high dimensions. One potential drawback is the gradient may not always be available. Since we have an estimate of $\nabla_\theta \ell(\theta)$ following Proposition 3.1, and hence of $\nabla_\theta U(\theta)$, we consider a candidate θ' constructed using reflected Hamiltonian dynamics (Betancourt, 2011), so that $\theta' \in \Theta$. This proposal is then finally accepted with a Metropolis-Hastings correction (Neal et al., 2011, Equation 3.6). To complete the algorithmic specifications, in low-dimensional situations, we use a flat Gaussian prior (mean 0 and variance 100) on the parameters for Ising model. For PGM, we use Gaussian priors on the diagonal elements of θ (same parameters as Ising) and a flat exponential prior on the off-diagonal elements (rate 0.01).

4.2 Penalized MLE and Bayesian inference in high dimensions

The more practically useful and statistically challenging situation arises when p is moderate to high-dimensional. We consider the problem of structure learning under the assumption of a sparse underlying graph G . This problem was considered by [Meinshausen and Bühlmann \(2006\)](#) within the context of Gaussian graphical models, [Ravikumar et al. \(2010\)](#) addressed Ising models, and [Yang et al. \(2012\)](#) for general PEGMs. All these approaches are based on the idea of neighborhood selection, wherein neighbors of each node are estimated separately. Essentially, these procedures rely on the pseudo-likelihood $\prod_{j=1}^p p_{\theta}(X_j | X_{-j})$ with a suitable penalty. To our knowledge, joint structure learning for general PEGMs has not been considered before. Let $\|M\|_1 = \sum_j \sum_k |M_{jk}|$ denote the ℓ_1 -norm of the matrix M . We propose the following ℓ_1 -penalized estimator for θ :

$$\hat{\theta}_{\lambda} = \arg \min_{\theta \in \Theta} -\ell(\theta) + \lambda \|\theta\|_1 = \arg \min_{\theta \in \Theta} Q(\theta). \quad (7)$$

For computing the estimator, a proximal optimization algorithm ([Parikh and Boyd, 2014](#)) can be used with minor modifications from the updates in (6). Indeed, the objective function is equivalent to $Q(\theta) + \mathbb{1}_{\theta \in \Theta}$. Since both the ℓ_1 -penalty and the parameter space Θ are convex, proximal maps of the sum of the two functions amount to the composition of the proximal maps of the functions ([Yu, 2013](#)). This leads to batch updates of the form:

$$\theta^{(t+1)} = \mathcal{P}_{\Theta} [\text{prox}_{\ell_1}(\theta^{(t)} + \gamma \nabla_{\theta} \ell(\theta^{(t)}))], \quad (8)$$

where $\text{prox}_{\ell_1}(x)$ is the well-known soft-thresholding operator applied to each element of x ([Parikh and Boyd, 2014](#)). The tuning parameter λ is selected via cross-validation wherein the out-of-sample log-likelihood is maximized. This usually results in better Frobenius norms but poor structure learning. When structure learning is the main focus, we estimate the underlying graph by averaging estimates \hat{G}_{λ} obtained over a grid of values for λ . A more detailed discussion is deferred to Supplementary Section S.3.

Fully Bayesian inference is also possible in the high-dimensional case. Prior choices for sparse parameters is a well-developed field. One popular choice is the family of scale mixtures of normal prior which is elicited as $\theta_{jk} \mid \rho_{jk}^2, \tau^2 \stackrel{iid}{\sim} N(0, \rho_{jk}^2 \tau^2)$, $\rho_{jk} \stackrel{iid}{\sim} f$, $\tau \sim g$ for some choice of mixing distribution f and g . These are computationally beneficial (Bhattacharya et al., 2016) compared to the discrete mixture priors (Mitchell and Beauchamp, 1988; George and McCulloch, 1993), without compromising statistical accuracy (Bhattacharya et al., 2015; Chakraborty et al., 2020; Bhadra et al., 2017). Furthermore, posterior modes under these priors can be thought of as a penalized estimator of θ under the penalty $-\log \pi(\theta)$. In particular, when $\tau = 1$ and $\rho_{jk}^2 \mid \lambda \sim \text{Exp}(1/2\lambda^2)$ (Park and Casella, 2008), then $-\log \pi(\theta) = \lambda \|\theta\|_1$, the posterior mode of which is $\hat{\theta}_\lambda$ in (7). In our work, we choose this prior augmented by the hyperprior $\lambda \sim \text{Gamma}(a_\lambda, b_\lambda)$, i.e. if $\pi_L(\theta)$ denotes the joint prior over θ , it can be specified hierarchically as $\theta_{jk} \mid \rho_{jk}^2, \lambda \stackrel{iid}{\sim} N(0, \rho_{jk}^2 \lambda^{-1})$, $\rho_{jk}^2 \stackrel{iid}{\sim} \text{Exp}(1/2)$ and $\lambda \sim \text{Gamma}(a_\lambda, b_\lambda)$. Additionally, to respect the restriction that $\theta \in \Theta$, we truncate the prior $\pi(\theta)$ to $\{\theta : \theta \in \Theta\}$ so that our working prior is $\pi(\theta) \propto \pi_L(\theta) \mathbb{I}_{\theta \in \Theta}$. An HMC sampler can be designed aided by the scale mixture representation of $\pi(\theta)$. Indeed, the conditional log-posterior $U(\theta \mid \{\rho_{jk}\})$ is differentiable, and the HMC sampler can be implemented conditional on the latent $\{\rho_{jk}\}$. The latent $\{\rho_{jk}\}$'s can be updated given θ_{jk} using an inverse-Gaussian distribution. Details are given in Supplementary Section S.3.

5 Applications to Partially Observed Graphical Models: The Restricted and Full Boltzmann Machines

First consider the training of RBMs. The complete data model is Ising, which is a PEGM, and thus the proposed methodology can be used without much effort. To see this, consider the Expectation Maximization (EM) algorithm for computing the maximum likelihood estimator. Standard calculations yield the following updates for a gradient ascent algorithm

for the weights between the hidden and visible variables:

$$\begin{aligned} \theta^{(t+1)} &= \theta^{(t)} + \gamma \left\{ \mathbb{P}(\mathbf{h} = \mathbf{1} \mid \mathbf{v}, \theta = \theta^{(t)}) \mathbf{v}^T - \nabla_{\theta} \log z(\theta^{(t)}) \right\} \\ &= \theta^{(t)} + \gamma \left\{ \mathbb{P}(\mathbf{h} = \mathbf{1} \mid \mathbf{v}, \theta = \theta^{(t)}) \mathbf{v}^T - \mathbb{E}_{(\mathbf{h}, \mathbf{v}) \sim p_{\phi}} \left[\frac{\nabla_{\theta} e^{-E_{\theta}(\mathbf{v}, \mathbf{h})}}{e^{-E_{\phi}(\mathbf{v}, \mathbf{h})}} \right] \middle/ \mathbb{E}_{(\mathbf{h}, \mathbf{v}) \sim p_{\phi}} \left[\frac{e^{-E_{\theta}(\mathbf{v}, \mathbf{h})}}{e^{-E_{\phi}(\mathbf{v}, \mathbf{h})}} \right] \right\}, \end{aligned} \quad (9)$$

where the second equality follows from Proposition 3.1. For RBMs, $\mathbb{P}(\mathbf{h} = \mathbf{1} \mid \mathbf{v}, \theta = \theta^{(t)}) = \prod_{k=p+1}^{p+m} \mathbb{P}(h_k = 1 \mid \mathbf{v}, \theta = \theta^{(t)})$, which is a product of sigmoid functions. Updates for the biases are similar. Similar to the CD algorithm described in Section 2.2, the proposed algorithm here also makes use of Monte Carlo sampling to estimate $\nabla_{\theta} \log z(\theta)$. But, unlike CD, in this case samples $(\mathbf{h}, \mathbf{v}) \sim p_{\phi}$ are independent, and estimates the correct gradient. A Gibbs sampler is not needed.

Remarkably, the proposed framework allows a feasible training method for a full BM as well; a problem long considered intractable. Define the parameter matrix $\theta \in \mathbb{R}^{(p+m) \times (p+m)}$ as $\theta = \begin{pmatrix} \theta_{\mathbf{pp}} & \theta_{\mathbf{pm}} \\ \theta_{\mathbf{pm}}^T & \theta_{\mathbf{mm}} \end{pmatrix}$, where $\theta_{\mathbf{pp}}$ contains bias and interaction terms between the visible variables, $\theta_{\mathbf{pm}}$ contains the interaction terms between the hidden variables, and $\theta_{\mathbf{mm}}$ contains bias and interaction terms between the hidden variables. At $\theta = \theta^{(t)}$, the expected value of the complete data log-likelihood given the observed \mathbf{v} is:

$$\begin{aligned} \mathbb{E}_{\theta^{(t)}, \mathbf{v}} \{ \log p_{\theta}(\mathbf{v}, \mathbf{h}) \} &= \sum_j \theta_{jj} v_j + \sum_k \theta_{kk} \mathbb{E}_{\theta^{(t)}, \mathbf{v}}(h_k) + \sum_{j \neq j'} \theta_{jj'} v_j v_{j'} \\ &\quad + \sum_{k \neq k'} \theta_{kk'} \mathbb{E}_{\theta^{(t)}, \mathbf{v}}(h_k h_{k'}) + \sum_{j, k} \theta_{jk} v_j \mathbb{E}_{\theta^{(t)}, \mathbf{v}}(h_k) - \log z(\theta), \end{aligned}$$

for $j, j' = 1, \dots, p$; $k, k' = p+1, \dots, p+m$, where $\mathbb{E}_{\theta^{(t)}, \mathbf{v}}$ stands for the expectation taken with respect to the density $p_{\theta^{(t)}}(\cdot \mid \mathbf{v})$. Thus, to train this model using EM, one needs $\{ \mathbb{E}_{\theta^{(t)}, \mathbf{v}}(h_k), \mathbb{E}_{\theta^{(t)}, \mathbf{v}}(h_k h_{k'}) \}$, or more generally, $\mathbb{E}_{\theta^{(t)}, \mathbf{v}} \{ g(\mathbf{h}) \}$, where $g(\mathbf{h}) = g(h_1, \dots, h_m)$ is a function of the hidden variables. Fortunately, the conditional distribution of $\mathbf{h} \mid \mathbf{v}$, i.e.

$p_\theta(\cdot | \mathbf{v})$ here is also Ising. Indeed,

$$p_{\theta_{\mathbf{h}|\mathbf{v}}}(\mathbf{h} | \mathbf{v}) \propto \exp \left\{ \sum_k (\theta_{kk} + \sum_j \theta_{jk} v_j) h_k + \sum_{k \neq k'} \sum \theta_{kk'} h_k h_{k'} \right\} = \exp(-E_{\theta_{\mathbf{h}|\mathbf{v}}}(\mathbf{v}, \mathbf{h})),$$

where the notation $\theta_{\mathbf{h}|\mathbf{v}}$ stands for the parameter of the conditional Ising model for $\mathbf{h} | \mathbf{v}$.

A self-normalized importance sampling estimate of $\mathbb{E}_{\theta, \mathbf{v}}\{g(\mathbf{h})\}$ is now presented.

Proposition 5.1. *Define $w(\mathbf{v}, \mathbf{h}) = \exp\{-E_{\theta_{\mathbf{h}|\mathbf{v}}}(\mathbf{v}, \mathbf{h}) + E_{\phi_{\mathbf{h}|\mathbf{v}}}(\mathbf{v}, \mathbf{h})\}$. Then,*

$$\mathbb{E}_{\theta, \mathbf{v}}\{g(\mathbf{h})\} = \mathbb{E}_{(\mathbf{h}|\mathbf{v}) \sim \phi_{\mathbf{h}|\mathbf{v}}} \left[g(\mathbf{h}) \frac{p_{\theta_{\mathbf{h}|\mathbf{v}}}(\mathbf{h} | \mathbf{v})}{p_{\phi_{\mathbf{h}|\mathbf{v}}}(\mathbf{h} | \mathbf{v})} \right] = \frac{\mathbb{E}_{(\mathbf{h}|\mathbf{v}) \sim \phi_{\mathbf{h}|\mathbf{v}}} [g(\mathbf{h})w(\mathbf{v}, \mathbf{h})]}{\mathbb{E}_{(\mathbf{h}|\mathbf{v}) \sim \phi_{\mathbf{h}|\mathbf{v}}} [w(\mathbf{v}, \mathbf{h})]},$$

where a natural choice for $\phi_{\mathbf{h}|\mathbf{v}}$ is $\text{diag}(\theta_{\mathbf{h}|\mathbf{v}})$.

Proof. Clearly,

$$\mathbb{E}_{(\mathbf{h}|\mathbf{v}) \sim \phi_{\mathbf{h}|\mathbf{v}}} \left[g(\mathbf{h}) \frac{p_{\theta_{\mathbf{h}|\mathbf{v}}}(\mathbf{h} | \mathbf{v})}{p_{\phi_{\mathbf{h}|\mathbf{v}}}(\mathbf{h} | \mathbf{v})} \right] = \mathbb{E}_{(\mathbf{h}|\mathbf{v}) \sim \phi_{\mathbf{h}|\mathbf{v}}} [g(\mathbf{h})w(\mathbf{v}, \mathbf{h})] \left[\frac{z(\theta_{\mathbf{h}|\mathbf{v}})}{z(\phi_{\mathbf{h}|\mathbf{v}})} \right]^{-1}.$$

The proof follows by applying (5) to the second term on the right hand side of the above. \square

Remark 5.1. *Variance of this self-normalized importance sampling estimate is finite when $\phi_{\mathbf{h}|\mathbf{v}} = \text{diag}(\theta_{\mathbf{h}|\mathbf{v}})$. Indeed, the estimator Z is of the form $Z = X/Y$. Thus, the Cauchy-Schwarz inequality gives $\text{Var}_{\phi_{\mathbf{h}|\mathbf{v}}}(Z) \leq \mathbb{E}_{\phi_{\mathbf{h}|\mathbf{v}}}(X^2/Y^2) \leq \mathbb{E}_{\phi_{\mathbf{h}|\mathbf{v}}}(X^2)\mathbb{E}_{\phi_{\mathbf{h}|\mathbf{v}}}(1/Y^2)$. Since $g(\mathbf{h})$ is bounded for $g(\mathbf{h}) = h_k$ and $g(\mathbf{h}) = h_k h_{k'}$; $k, k' = p+1, \dots, p+m$; another application of Cauchy-Schwarz inequality along with Proposition 3.2 proves that $\mathbb{E}_{\phi_{\mathbf{h}|\mathbf{v}}}(X^2) < \infty$. The random denominator $1/Y$ is of the form $\exp\{E_{\theta_{\mathbf{h}|\mathbf{v}}}(\mathbf{v}, \mathbf{h}) - E_{\phi_{\mathbf{h}|\mathbf{v}}}(\mathbf{v}, \mathbf{h})\}$. That the variance of this quantity is finite follows from Proposition 3.2.*

Remark 5.2. *The key difference between training a BM and an RBM is that when using (9) for RBMs, one Monte Carlo estimate of $z(\theta)$ is sufficient. However, for BMs, Monte Carlo estimates of $\mathbb{E}_{\theta, \mathbf{v}}\{g(\mathbf{h})\}$ are needed. Moreover, the parameters of $\mathbf{h} | \mathbf{v}$ are dependent on \mathbf{v} . A CD-type algorithm can in principle be implemented, but would be immensely expensive since one needs to run an m -dimensional Gibbs sampler for each \mathbf{v} . On the*

other hand, with the proposed method, batch sampling is possible using the specific choice $\phi_{\mathbf{h}|\mathbf{v}} = \text{diag}(\theta_{\mathbf{h}|\mathbf{v}})$.

Remark 5.3. *The training of BM also allows one to compute an estimate of the marginal likelihood of the visible variables. Indeed, for all $\mathbf{h} \in \{0, 1\}^m$, the following relation holds: $\log p_{\hat{\theta}}(\mathbf{v}) = \log p_{\hat{\theta}}(\mathbf{v}, \mathbf{h}) - \log p_{\hat{\theta}}(\mathbf{h} | \mathbf{v})$. Since both (\mathbf{v}, \mathbf{h}) and $(\mathbf{h} | \mathbf{v})$ are Ising, this quantity is computable using techniques developed here. The marginal likelihood may then be used for model selection or hyperparameter tuning purposes.*

The proposed framework also encompasses the DBM where there are multiple layers of hidden variables but the underlying graph can be rearranged in a two-layer graph (Aggarwal, 2018), with all odd layer variables constituting one half of the graph and even layers constituting the other half, with the restriction that connections between variables in the same layer are not allowed; see Figure 1. Thus, the DBM can be thought of as a relaxation of the BM and a similar training algorithm can be implemented in principle to train the model. We omit the details. In the context of DBM, Salakhutdinov and Murray (2008) proposed a related annealed importance sampling scheme (Neal, 2001) where a similar choice of $\phi = \text{diag}(\theta)$ is proposed for computing marginal probabilities. But they do not discuss full likelihood inference, and still train their model via CD.

6 Theoretical Properties

In this section we investigate the properties of the likelihood-based estimates, including the Bayesian posterior, specifically in high-dimensional settings, since the properties of these procedures in low-dimensional problems are fairly well-understood. We first focus on the ℓ_1 -penalized estimator in (7). Since its introduction in the regression context (Tibshirani, 1996), ℓ_1 -penalized estimators have been used in many other settings; for instance in sparse covariance estimation problems (Rothman et al., 2010), reduced-rank prob-

lems (Yuan et al., 2007), generalized linear models (Ravikumar et al., 2010; Yang et al., 2012), among others. These estimators have been shown to be consistent with the optimum rate of convergence for sparse problems. We establish these properties of the estimator in (7) for PEGMs under fairly general assumptions, drawing parallels with the existing literature. In the sequel, we write $\theta_0 \in \Theta$ as the true data-generating parameter, and $\mathbf{S} = \{(j, k) : \theta_{0,jk} \neq 0, j, k = 1, \dots, p\}$, $|\mathbf{S}| = s$. We start by stating the assumptions.

Assumption 6.1 (Dimension). *We assume that $\log p = o(n)$, $s = o(p)$ and $s \log p = o(n)$ where $a_n = o(b_n)$ denotes $a_n/b_n \rightarrow 0$ as $n \rightarrow \infty$.*

Assumption 6.2 (Regularity). *The space Θ of feasible parameters is open and θ_0 is in the interior of Θ . We also assume the PEGM is sufficiently regular, i.e., for some $\beta, \rho > 0$,*

$$\lambda_{\min} \left(\frac{\partial^2}{\partial \theta^2} A(\theta_0) \right) \geq \beta, \quad \left[\sum_{j,k,l=1}^p \left(\frac{\partial^3}{\partial \theta^3} A(\theta_0) \right)_{jkl}^2 \right]^{1/2} \leq \rho,$$

where λ_{\min} denotes the minimum eigenvalue.

Assumption 6.3 (Bounded moments). *For all $j, k = 1, \dots, p$, assume, $\mathbb{E}_{\theta_0}[|T(X_j)|] \leq \kappa_1$, $\mathbb{E}_{\theta_0}[T^2(X_j)] \leq \kappa_2$, and $\mathbb{E}_{\theta_0}[|T(X_j, X_k)|] \leq \kappa_3$. Also, assume that,*

$$\max_{u:|u|<1} \frac{\partial^2}{\partial \theta_j^2} A(\theta_0 + ue_j) \leq \kappa_4,$$

where $e_j \in \mathbb{R}^p$ is the unit vector corresponding to the index j . Assume, furthermore,

$$\max_{\eta:|\eta|<1} \frac{\partial^2}{\partial \eta^2} \bar{A}_{jk}(\theta_0; \eta) \leq \kappa_5,$$

where,

$$\bar{A}_{jk}(\theta; \eta) := \log \int_{\mathcal{X}} \exp \left\{ \eta T(X_j, X_k) + \sum_{j=1}^p \theta_j T(X_j) + \sum_{j \neq k=1}^p \theta_{jk} T(X_j, X_k) + \sum_{j=1}^p C(X_j) \right\} dx.$$

Assumption 6.2 imposes the condition that the covariance matrix of the model is not singular and can be reasonably well approximated within a small neighborhood of θ_0 . As-

sumption 6.3 controls the size of the deviations of the sample moments from the population moments. Then we have the following result, with a proof in Supplementary Section S.1.4.

Theorem 6.4. *Suppose we observe n i.i.d copies $\mathbf{X} = (X_{1\bullet}, \dots, X_{n\bullet}) \sim \text{PEGM}(\theta)$. Let $r_n = \sqrt{\frac{s \log p}{n}}$ and $\hat{\theta}_\lambda$ be a solution to (7). Under Assumptions 6.1–6.3, for $\lambda \asymp \sqrt{\frac{\log p}{n}}$, there exists sufficiently large $M > 0$ such that as $n \rightarrow \infty$, one has:*

$$\mathbb{P}_{\theta_0} \left[\left\| \hat{\theta}_\lambda - \theta_0 \right\|_F^2 > Mr_n \right] \rightarrow 0,$$

where $\|\cdot\|_F$ denotes the Frobenius norm.

The rate of convergence of the ℓ_1 -penalized estimator matches with existing rates in sparse parameter estimation theory; see for example Rothman et al. (2010).

Frequentist evaluation of Bayesian posteriors is typically studied through the lens of posterior consistency and contraction rates (Ghosal and Van der Vaart, 2017). In models with increasing number of parameters, a standard condition for posterior consistency is positive prior support on shrinking Kullback–Liebler balls around the true distribution. Suppose p_{θ_0} is the true distribution of the data and p_θ is the fitted distribution. Let $\pi(\theta)$ be the prior distribution on θ and $\text{KL}(p_{\theta_0}, p_\theta)$ denote the Kullback–Liebler divergence between p_{θ_0} and p_θ . In Proposition S.1.2, we show when p_{θ_0} and p_θ are PEGMs, then the set $\{\theta : \text{KL}(p_{\theta_0}, p_\theta) < \epsilon\}$ for any $\epsilon > 0$ can be characterized in terms of $\|\text{vech}(\theta_0) - \text{vech}(\theta)\|_2^2$, where $\text{vech}(\theta)$ stands for the half-vectorization of a symmetric matrix θ . As a result, any prior distribution that has positive mass on the set $\{\theta : \|\text{vech}(\theta_0) - \text{vech}(\theta)\|_2^2 < \epsilon\}$ for $\epsilon > 0$ yields a consistent posterior. Properties of global-local shrinkage priors around small Euclidean neighborhoods of a sparse parameter are well studied; see, e.g., Bhattacharya et al. (2016). We next establish posterior consistency for PEGMs under prior $\pi(\theta) \propto \pi_L(\theta)\mathbb{I}_{\theta \in \Theta}$ where $\pi_L(\theta)$ is defined at the end of Section 4.2.

Theorem 6.5. *Suppose we observe n i.i.d copies $\mathbf{X} = (X_{1\bullet}, \dots, X_{n\bullet}) \sim \text{PEGM}(\theta)$ and θ is endowed with prior $\pi(\theta) \propto \pi_L(\theta)\mathbb{I}_{\theta \in \Theta}$ where $\pi_L(\theta)$ is the marginal prior obtained*

under hierarchy $\theta_j \mid \lambda \stackrel{iid}{\sim} \text{Laplace}(\lambda^{-1})$ and $\lambda \sim \text{Gamma}(a_\lambda, b_\lambda)$. If, $a_\lambda = O(s \log p)$ and $b_\lambda = O\left(s \sqrt{\frac{s \log p}{np}}\right)$, then, under Assumptions 6.1–6.3, for every sufficiently small $\epsilon > 0$, we have in \mathbb{P}_{θ_0} -probability:

$$\pi [\theta : \|\theta - \theta_0\|_F > \epsilon \mid \mathbf{X}] \rightarrow 0.$$

See Supplementary Section S.1.5 for a proof. We next turn our attention to partially observed models, specifically the RBM. Suppose we observe n i.i.d variables $\mathbf{V} = (\mathbf{v}_{1\bullet}, \dots, \mathbf{v}_{n\bullet})^\top$ with support on $\{0, 1\}^p$. When an RBM is fitted to the observed data, maximum likelihood inference involves optimizing the marginal likelihood (4). The iterative scheme (9) essentially performs Monte Carlo EM algorithm on the complete-data log-likelihood. Let $Q(\theta; \psi) = \mathbb{E}_\psi[-E_\theta(\mathbf{v}, \mathbf{h})] - \log z(\theta) = g(\mathbf{v}; \theta, \psi) - \log z(\theta)$, and $Q^*(\theta; \psi) = g(\mathbf{v}; \theta, \psi) - \widehat{\log z(\theta)}$, its Monte Carlo estimate. Our next result shows EM sequences based on $Q(\theta; \psi)$ and $Q^*(\theta; \psi)$ are not far apart. The proof is given in Supplementary Section S.1.6.

Theorem 6.6. *Let the parameter space Θ be compact. Suppose $\{\theta^{(t)}\}$ is a generalized EM sequence obtained with initial point $\theta^{(0)}$, step sizes γ_t , and let this sequence converge to a stationary point $\underline{\theta}$ of (4), i.e. $\nabla \log p_\theta(\mathbf{v})|_{\theta=\underline{\theta}} = 0$. Also, assume that $\gamma_t \lambda_{\max}[\nabla_{\theta\theta}^2 g(\mathbf{v}; \theta; \psi)] + \gamma_t \lambda_{\max}[\nabla^2 \log z(\theta)] \leq 1$ for all $t \geq 1$ and $\theta \in \Theta$, and $\sum_{t=1}^\infty \gamma_t = 0$. Let $\theta_\star^{(t)}$ denote a sequence with the same initial point and step-sizes obtained using $Q^*(\theta; \psi)$. Then for sufficiently large t ,*

$$\|\theta^{(t)} - \theta_\star^{(t)}\|_F = O\left(\frac{1}{t^{1+\eta}}\right),$$

for some $\eta > 0$, $\mathbb{P}_{\theta_\star^{(1)}} \otimes \dots \otimes \mathbb{P}_{\theta_\star^{(t)}}$ -almost surely.

7 Numerical Experiments

We compare the performances of (maximum) likelihood based methods (MLE), including a full Bayes method, to that of (maximum) pseudo-likelihood (MPLE) based methods for parameter inference in PEGMs. We consider the Ising model and the PGM as examples

of PEGMs. We design our experiment in a low-dimensional (LD), high-dimensional (HD), and ultra high-dimensional (UHD) setting for both models. In the low-dimensional setting, our goal is to demonstrate the efficiency in terms of uncertainty quantification of a full likelihood based analysis since both MLE and PMLE are consistent. The focus in the (ultra) high-dimensional setting is to understand the performance of *penalized* versions of these methods, PMLE and PMPLE, respectively, in terms of graph structure learning. We set the dimension $p = 3, 5$ (low-dimensional) and $p = 20, 30, 40, 50$ (high-dimensional) and $p = 100, 200, 300$ (ultra high-dimensional). For both low and high-dimensional settings, the sample size is set as $n = 100$. In the ultra high-dimensional setting we set $n = 2p$. The true parameter θ_0 for all the cases is generated randomly, first by sampling $z_{jk} \sim \text{Bernoulli}(\omega)$ and then setting $\theta_{0,jk} | [z_{jk} = 0] = 0$ and $\theta_{0,jk} | [z_{jk} = 1] = \eta$. In the low-dimensional setting we set $\omega = 0.9$, $\eta = -0.8$, whereas for the other two cases we set $\omega = 0.05$, $\eta = -3$.

In the LD setting, we compare the methods using the Frobenius norm $\|\hat{\theta} - \theta_0\|_F^2$, average coverage probabilities of 95% confidence intervals, and their corresponding widths. For the Bayes method, we choose $\hat{\theta}$ as the posterior mean using the Laplace scale mixture prior described previously. In the HD setting, we focus on the Matthews correlation coefficient (MCC) (Chicco et al., 2021) between the estimated and the true graph and $\|\hat{\theta} - \theta_0\|_F^2$. The MCC values ranges between -1 and $+1$, with -1 indicating the worst performance and $+1$ the best. The advantage of MCC as a measure is that its value is close to $+1$ if and only if the estimated graph estimates zero and non-zero edges between nodes correctly at the same time. We only consider PMLE and PMPLE here, since the Bayesian posterior mean with a continuous shrinkage prior is not sparse. For both of these methods, the estimated graph is produced following the procedure described in Supplementary Section S.3. Additionally, we report $\|\hat{\theta} - \theta_0\|_F^2$, where for PMLE, the estimate $\hat{\theta}$ correspond to the one obtained using cross-validation. Finally, in the UHD setting, we only consider MCC of PMLE and PMPLE. We summarize the Frobenius norm and MCC for the Ising model and PGM in

			Ising				PGM					
Setting	p	n	$\ \theta_0 - \hat{\theta}\ _F^2$			MCC		$\ \theta_0 - \hat{\theta}\ _F^2$			MCC	
			PMLE	PMPLE	Bayes	PMLE	PMPLE	PMLE	PMPLE	Bayes	PMLE	PMPLE
LD	3	100	1.24 (0.52)	6.48 (6.05)	2.09 (1.62)	–	–	0.38 (0.09)	5.83 (5.65)	0.70 (0.02)	–	–
	5		2.07 (0.85)	16.23 (6.42)	1.68 (0.28)	–	–	0.98 (0.27)	19.57 (5.21)	1.37 (0.30)	–	–
HD	20	100	9.18 (0.61)	9.56 (0.57)	10.58 (0.27)	0.67 (0.05)	0.48 (0.01)	11.60 (0.43)	13.62 (0.17)	13.91 (0.05)	0.83 (0.07)	0.24 (0.02)
	30		12.85 (0.99)	13.94 (0.61)	16.24 (0.38)	0.78 (0.02)	0.49 (0.02)	15.27 (1.25)	20.43 (0.12)	20.94 (0.01)	0.71 (0.05)	0.22 (0.02)
	40		18.61 (1.31)	27.38 (0.11)	24.33 (0.29)	0.71 (0.05)	0.46 (0.03)	21.00 (1.03)	27.06 (0.07)	27.26 (0.01)	0.73 (0.04)	0.25 (0.02)
	50		26.89 (0.50)	35.38 (0.09)	32.10 (0.21)	0.71 (0.03)	0.39 (0.03)	30.57 (1.32)	34.36 (0.15)	33.85 (0.01)	0.61 (0.04)	0.22 (0.02)
UHD	100	200	54.35 (0.93)	69.71 (0.04)	–	0.80 (0.02)	0.44 (0.01)	59.26 (0.62)	67.43 (0.07)	–	0.52 (0.02)	0.27 (0.01)
	200	400	128.97 (0.14)	137.16 (0.02)	–	0.70 (0.01)	0.41 (0.01)	131.84 (0.03)	134.70 (0.05)	–	0.47 (0.01)	0.34 (0.01)
	300	600	195.97 (0.06)	202.21 (0.02)	–	0.56 (0.01)	0.24 (0.01)	201.11 (0.03)	203.73 (0.05)	–	0.50 (0.01)	0.33 (0.01)

Table 1: Mean (sd) of $\text{MSE} = \|\hat{\theta} - \theta_0\|_F^2$ and Matthews correlation coefficient (MCC) across 10 datasets for penalized maximum likelihood estimation (PMLE), penalized maximum pseudo-likelihood estimation (PMPLE) and the Bayes methods for Ising and PGM.

Table 1 for 10 replications. The average coverage probabilities of 95% confidence intervals and their corresponding widths for both models in the LD settings are in Supplementary Table S.1. Full likelihood-based methods achieve lower Frobenius norms in all the settings considered, for both Ising and PGM, compared to their PMPLE counterparts. In terms of graph reconstruction, the PMLE estimator (7) outperforms the PMPLE-based methods with significantly higher MCC values. Figure 2 shows the heatmap comparing the data generating parameter θ_0 and the estimates obtained from PMPLE and PMLE for the Ising model with $p = 20$; the PMLE estimate corresponds to $\lambda = 7$. Clearly, $\hat{\theta}_{PMPLE}$ effectively captures the underlying structure and also yields estimates that are closer to the truth. Finally, we note that penalization was not used in LD, and the fully Bayesian procedure was computationally prohibitive in UHD. These cases are marked with a ‘–’ in Table 1. Additional simulation results on the partially observed case, comparing the representational powers of BM and RBM, are presented in Supplementary Section S.4.2.

8 Data Analysis

We provide demonstrations on data sets arising from disparate applications, intentionally so chosen, to demonstrate the scope of the methodology.

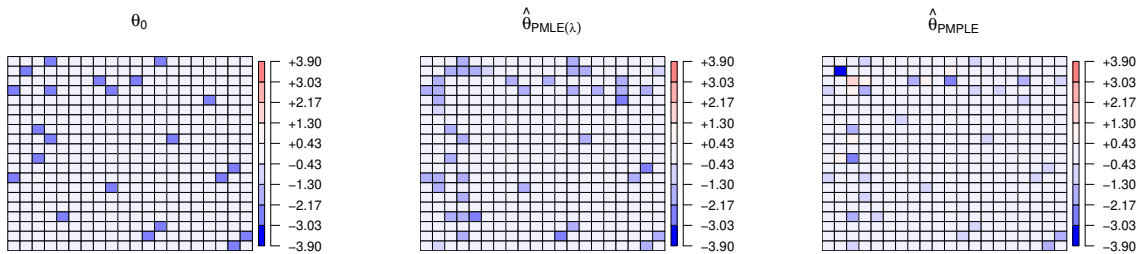


Figure 2: True parameter θ_0 and the corresponding PMLE and PMPLE estimates $\hat{\theta}$ for the Ising model with $(n, p) = (100, 20)$ and $\lambda = 7$.

8.1 Movie ratings network via Ising model

We demonstrate the merits of a likelihood-based analysis for the Ising Model by analyzing a real-world movie rating dataset. The original *Movielens 25M* dataset collected by Grouplens consists of movie ratings, ranging from 0 to 5 with increments of 0.5, for 62,000 movies by 162,000 users (<https://grouplens.org/datasets/movielens/>). We select the most frequently rated 50 movies ($p = 50$) from the same group of $n = 303$ viewers. We code observations that received a rating of 5 as ‘1’, signifying complete satisfaction with the film, and assign ‘0’ to ratings of 4.5 or below (Roach and Gao, 2023). Supplementary Table S.3 provides the legend of the movie titles, genres, and years of release. The binary variables X_{ij} indicates the preference of the i th viewer for the j th movie, where $i = 1, \dots, 303$ and $j = 1, \dots, 50$. Specifically, $X_{ij} = X_{ik} = 1$, where $j \neq k$, implies that the i th viewer has strong preference for both movies j and k . Other combinations can also be interpreted similarly. We model the distribution of X using $\text{Ising}(\theta)$ where $\theta \in \mathbb{R}^{p \times p}$. Diagonal elements of θ model the propensity of a movie being rated 1, whereas off-diagonal elements capture the direction of association between movies (j, k) conditional on other movies.

We estimate θ using (7) and build the graph structure using the stable selection algorithm described in the Supplementary Section S.3. For stable selection, we select a grid of values of $\lambda = 5, 10, \dots, 100$ and set threshold $\pi_{thr} = 0.6$. The resulting movie rating network with abbreviations of the movie titles is plotted in Supplementary Figure S.2,

Positive Edge	$\hat{\theta}_{jk}$	Negative Edge	$\hat{\theta}_{jk}$
Lord of the Rings (2003) - Lord of the Rings (2001)	0.77	Inception (2010) - Batman (1989)	-0.95
Lord of the Rings (2002) - Lord of the Rings (2001)	0.72	Terminator (1984) - Dances with Wolves (1990)	-0.80
Lord of the Rings (2003) - Lord of the Rings (2002)	0.61	True Lies (1994) - Star Wars: Episode IV (1977)	-0.53
Star Wars: Episode V (1980) - Star Wars: Episode IV (1977)	0.56	Memento (2000) - Fugitive (1993)	-0.49
Terminator (1984) - Terminator 2: Judgment Day (1991)	0.55	Inception (2010) - Terminator (1984)	-0.48
Star Wars: Episode VI (1983) - Star Wars: Episode IV (1977)	0.53	Dances with Wolves (1990) - Twelve Monkeys (1995)	-0.44
Star Wars: Episode VI (1983) - Star Wars: Episode V (1980)	0.48	Independence Day (1996) - Batman (1989)	-0.44
Raiders of the Lost Ark (1981) - Star Wars: Episode V (1980)	0.40	Godfather (1972) - Independence Day (1996)	-0.42
Godfather (1972) - Schindler's List (1993)	0.25	Inception (2010)-Independence Day (1996)	-0.41
Raiders of the Lost Ark (1981) - Star Wars: Episode IV (1977)	0.24	Braveheart (1995) - Toy Story (1995)	-0.39

Table 2: Top 10 positive and negative interactions in the Movie Ratings Network.

where the edge widths are proportional to the stable selection probability, and the node sizes are proportional to the degree. Our analysis reveals that *Star Wars IV* and *Star Wars V* have the most connections, partly due to their appeal to a broader audience, see Supplementary Table S.4. *Lord of the Rings: The Fellowship of the Ring* has the second most connections. These two movie franchise also form two separate cliques within the graph, see Supplementary Figure S.2. A more detailed summary of the results, in terms of the most positive and negative connections, is provided in Table 2. Movies within the *Lord of the Rings* and *Star Wars* franchises have strong positive connections, whereas *Inception (2010)* and *Batman (1989)* have the strongest negative connection. We remark here that *Batman (1989)* is directed by Tim Burton, unlike the popular Batman movie franchise of the 2000s directed by Christopher Nolan, who also directed *Inception (2010)*. A heatmap of $\hat{\theta}_\lambda$ for $\lambda = 10$ is in Supplementary Figure S.3.

8.2 Breast cancer microRNA network via Poisson graphical model

We next apply a full-likelihood ($\hat{\theta}_{PMLE}$) and pseudo-likelihood ($\hat{\theta}_{PMPL}$) analysis to the task of inferring dependency among count-valued variables that represent microRNA (miRNA) expression profiles of the 353 genes. This level III RNA-Seq data is collected from 445 breast invasive carcinoma (BRCA) patients ($n = 445$) from the Cancer Genome Atlas (TCGA) project (TCGA, 2012) and is available in the R package **XMRF**. The observed values are counts of sequencing reads mapped back to a reference genome. Raw counts are highly

skewed and zero-inflated. We use the `processSeq` function in the `XMRP` package to adjust for sequencing depth, mitigate overdispersion, and normalize the counts. Since the PGM can only model negative conditional associations, we select a subset of $p = 101$ genes with negative Pearson correlation between their counts.

We select a grid of $\lambda_{PMLE} = [200, 240, 280, \dots, 1000]$, and set the threshold $\pi_{thr} = 0.6$ to implement the stable selection algorithm. For pseudo-likelihood, we perform node-wise ℓ_1 penalized Poisson generalized linear model (GLM) using `glmnet` (Friedman et al., 2010) in R with a negative constraint on coefficients and consider a grid of 20 evenly spaced values in the interval $[5\sqrt{\log p/n}, 7\sqrt{\log p/n}]$ for the penalty parameter λ_{PMLE} . We then construct the final estimator $\hat{\theta}_{\lambda, PMLE}$ for a given λ by setting $\hat{\theta}_{\lambda, PMLE} = (\hat{\theta}_{\lambda} + \hat{\theta}_{\lambda}^x)/2$, where $\hat{\theta}_{\lambda}$ represents the matrix formed by coefficients from Poisson GLMs. The sequence of estimates $\hat{\theta}_{\lambda, PMLE}$ are then used for model selection following the stable selection procedure with $\pi_{thr} = 0.6$.

Estimated networks from a full-likelihood and pseudo-likelihood based analysis are comparable. Supplementary Figures S.4 and S.5 show the estimated networks from a likelihood and pseudo-likelihood analysis, respectively, where blue edges are common to both networks. Let $S_{PMLE} := \{(j, k) : \hat{\theta}_{PMLE, jk} \neq 0, 1 \leq j \leq k \leq p\}$ and $S_{PMPLE} := \{(j, k) : \hat{\theta}_{PMPLE, jk} \neq 0, 1 \leq j \leq k \leq p\}$. The cardinality of the intersection $|S_{PMLE} \cap S_{PMPLE}| = 372$ is about 70% of $|S_{PMLE}|$. Moreover, the genes with the top numbers of connections in the PMLE-based network also have high degrees of rank in the PMPLE-based network, as shown in Table 3. Both networks successfully identify the edge between the CDH1 (located on chromosome 16q) and the BCL9 (located on chromosome 1q). Existing studies reported that the CDH1 is often underexpressed, while the BCL9 is typically overexpressed, caused by frequent chromosomal aberrations involved in breast cancer pathogenesis (Privitera et al., 2021). Additionally, the top connected genes in Table 3, such as WHSC1L1, TMPRSS2, CDH1, SLC34A2 and EP300, are all known key players in breast

cancer (Xiao et al., 2022; Kim et al., 2021).

Gene	WHSC1L1	TMPRSS2	CDH1	SLC34A2	FGFR2	EP300	RNF43	NUP98	ACSL3	MAP2K1
d_{PMLE} (Ranking)	52 (1)	36 (2)	24 (3)	21 (4)	21 (5)	20 (6)	19 (7)	19 (8)	19 (9)	19 (10)
d_{PMPLLE} (Ranking)	33 (3)	15 (43)	34 (2)	26 (7)	19 (25)	17 (32)	20 (21)	17 (32)	14 (49)	7 (84)

Table 3: Top 10 genes ranked by degrees from the full-likelihood based (d_{PMLE}) and pseudo-likelihood based (d_{PMPLLE}) estimates for Breast Cancer data.

8.3 Analysis of MNIST data via restricted and full Boltzmann machines

We analyze the MNIST data (Deng, 2012) using RBM and BM where we train the model with the proposed algorithm. The data consists of images of handwritten digits (0–9). The number of training samples for the 10 digits vary within the range $n = 3000$ to $n = 4000$. We consider images of 15×15 resolution. Each image is then converted to a binary vector of length $p = 225$, with on pixels are coded as 1 and off pixels are coded as 0. A fitted RBM or BM model on these images approximates the distribution of this binary vector over $\{0, 1\}^{225}$. Furthermore, since both RBM and BM are generative models, the trained models can be used to produce synthetic data based on held out test images of these digits. This is known as reconstruction. A well-trained model will generally capture the global distribution of the pixels for each digit, and be able to reproduce subject-specific variations within this global distribution. In Figure 3, we show the reconstructed images of test images for all the digits 0–9 with $m = 50$ hidden variables for both RBM and BM. Additionally, we compare the performance of reconstructed test images in terms of Brier loss. The Brier loss measures how well-calibrated the reconstructed probabilities are. This is done on test images of all the digits. Given a test image \mathbf{v} , and reconstructed probabilities $\hat{\mathbf{v}}$, we compute the Brier loss as

$$B = (n_t p)^{-1} \sum_{i=1}^{n_t} \sum_{j=1}^p (\mathbf{v}_{ij} - \hat{\mathbf{v}}_{ij})^2,$$

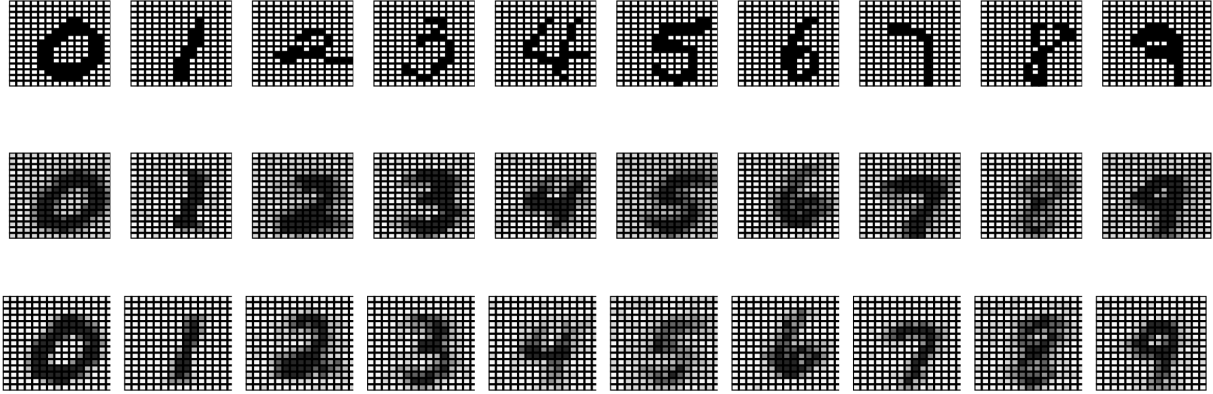


Figure 3: Observed and reconstructed images of handwritten digits. The first row corresponds to observed of test images of digits 0–9. The second and third rows show the reconstructed images from the trained RBM-MLE and BM-MLE model. All models are fitted with $m = 50$ hidden variables.

Digit	0	1	2	3	4	5	6	7	8	9
RBM-MLE	0.39	0.17	0.31	0.45	0.32	0.40	0.43	0.35	0.41	0.32
RBM-CD	0.44	0.36	0.42	0.48	0.43	0.43	0.47	0.39	0.41	0.40
BM-MLE	0.42	0.15	0.29	0.46	0.30	0.41	0.43	0.32	0.39	0.28

Table 4: Brier loss for RBM and BM trained with proposed algorithm and RBM trained with CD. The results demonstrate the superiority of full-likelihood based training over CD-based training.

where n_t is the number of test images. The results are reported in Table 4. Performance of the likelihood trained RBM (RBM-MLE) is better than CD trained RBM for all digits. Also, with the same number of hidden variables, BM-MLE achieves a (marginally) lower reconstruction error compared to RBM-MLE in most cases.

9 Conclusions and Future Works

The overarching focus of the current paper has been on the development of computationally feasible likelihood-based inference procedures in intractable graphical models, and in particular for models that were long considered impermeable to such inference, e.g., Boltzmann machine-based architectures. Our theoretical results on likelihood-based inference complement the methodological contributions. A number of future investigations can be

considered. First, we only considered first order gradient-based methods for optimization. However, since we have a Monte Carlo estimate of the gradient, a quasi-Newton approach such as BFGS (see, e.g., [Broyden, 1970](#)) appears straightforward to develop and may have better convergence speed in practice compared to a first order gradient descent scheme. Second, the intractability of the normalizing constant also affects the computation of evidence or marginal likelihood, and makes model selection and comparison difficult. Although not explicitly considered in this work, it is a natural future step is to consider model selection problems in exponential family graphical models and to consider multiple connected graphs, where we envisage that the techniques developed in this paper will prove fruitful.

SUPPLEMENTARY MATERIAL

(a) *Supplementary Text*: contains proofs, algorithmic details, and additional results from simulations and data analysis.

(b) *Supplementary Code*: an R package to implement the methodology can be downloaded from <https://github.com/chenyujie1104/ExponentialGM> along with a README file.

References

- D. H. Ackley, G. E. Hinton, and T. J. Sejnowski (1985). A learning algorithm for Boltzmann machines. *Cognitive Science* **9**, 147–169.
- C. C. Aggarwal (2018). *Restricted Boltzmann Machines*, pages 235–270. Springer International Publishing, Cham.
- J. Ashford and R. Sowden (1970). Multi-variate probit analysis. *Biometrics* pages 535–546.
- O. Barndorff-Nielsen (1978). *Information and exponential families in statistical theory*. John Wiley & Sons.
- J. Besag (1974). Spatial interaction and the statistical analysis of lattice systems. *Journal of the Royal Statistical Society: Series B (Methodological)* **36**, 192–225.
- M. Betancourt (2011). Nested sampling with constrained Hamiltonian Monte Carlo. In *AIP Conference Proceedings*, volume 1305, pages 165–172. American Institute of Physics.

- A. Bhadra, J. Datta, N. G. Polson, and B. Willard (2017). The Horseshoe+ Estimator of Ultra-Sparse Signals. *Bayesian Analysis* **12**, 1105 – 1131.
- A. Bhattacharya, A. Chakraborty, and B. K. Mallick (2016). Fast sampling with Gaussian scale mixture priors in high-dimensional regression. *Biometrika* **103**, 985–991.
- A. Bhattacharya, D. B. Dunson, D. Pati, and N. S. Pillai (2016). Sub-optimality of some continuous shrinkage priors. *Stochastic Processes and their Applications* **126**, 3828 – 3842. In Memoriam: Evarist Giné.
- A. Bhattacharya, D. Pati, N. S. Pillai, and D. B. Dunson (2015). Dirichlet–Laplace priors for optimal shrinkage. *Journal of the American Statistical Association* **110**, 1479–1490.
- S. Boucheron, G. Lugosi, and O. Bousquet (2003). Concentration inequalities. In *Summer school on machine learning*, pages 208–240. Springer.
- C. G. Broyden (1970). The convergence of a class of double-rank minimization algorithms 1. general considerations. *IMA Journal of Applied Mathematics* **6**, 76–90.
- P. Bühlmann and S. Van De Geer (2011). *Statistics for high-dimensional data: methods, theory and applications*. Springer Science & Business Media.
- A. Chakraborty, A. Bhattacharya, and B. K. Mallick (2020). Bayesian sparse multiple regression for simultaneous rank reduction and variable selection. *Biometrika* **107**, 205–221.
- A. Chakraborty, R. Ou, and D. B. Dunson (2023). Bayesian inference on high-dimensional multivariate binary responses. *Journal of the American Statistical Association* **0**, 1–12.
- D. Chicco, N. Tötsch, and G. Jurman (2021). The matthews correlation coefficient (mcc) is more reliable than balanced accuracy, bookmaker informedness, and markedness in two-class confusion matrix evaluation. *BioData mining* **14**, 1–22.
- L. Deng (2012). The MNIST database of handwritten digit images for machine learning research. *IEEE Signal Processing Magazine* **29**, 141–142.
- A. Fischer and C. Igel (2012). An introduction to restricted Boltzmann machines. In *Progress in Pattern Recognition, Image Analysis, Computer Vision, and Applications: 17th Iberoamerican Congress, CIARP 2012, Buenos Aires, Argentina, September 3-6, 2012. Proceedings 17*, pages 14–36. Springer.

- R. A. Fisher (1922). On the mathematical foundations of theoretical statistics. *Philosophical transactions of the Royal Society of London, Series A* **222**, 309–368.
- J. H. Friedman, T. Hastie, and R. Tibshirani (2010). Regularization paths for generalized linear models via coordinate descent. *Journal of Statistical Software* **33**, 1–22.
- E. I. George and R. E. McCulloch (1993). Variable selection via gibbs sampling. *Journal of the American Statistical Association* **88**, 881–889.
- C. J. Geyer (1991). Markov chain Monte Carlo maximum likelihood. In *Computing Science and Statistics: Proc. 23rd Symposium of the Interface Foundation*, pages 156–163.
- C. J. Geyer and E. A. Thompson (1992). Constrained Monte Carlo maximum likelihood for dependent data. *Journal of the Royal Statistical Society: Series B* **54**, 657–683.
- S. Ghosal and A. Van der Vaart (2017). *Fundamentals of nonparametric Bayesian inference*, volume 44. Cambridge University Press.
- D. O. Hebb (1949). *The organization of behavior: A neuropsychological theory*. Wiley.
- G. E. Hinton (2002). Training products of experts by minimizing contrastive divergence. *Neural Computation* **14**, 1771–1800.
- G. E. Hinton (2007). Boltzmann machine. *Scholarpedia* **2**, 1668.
- G. E. Hinton, B. Sallans, and Z. Ghahramani (1998). A hierarchical community of experts. In *Learning in graphical models*, pages 479–494. Springer.
- J. J. Hopfield (1982). Neural networks and physical systems with emergent collective computational abilities. *Proceedings of the National Academy of Sciences* **79**, 2554–2558.
- E. Ising (1924). *Beitrag zur theorie des ferro-und paramagnetismus*. PhD thesis, Grefe & Tiedemann Hamburg.
- H.-S. Kim et al. (2021). High whsc111 expression reduces survival rates in operated breast cancer patients with decreased cd8+ t cells: machine learning approach. *Journal of Personalized Medicine* **11**, 636.
- S. L. Lauritzen (1996). *Graphical models*, volume 17. Clarendon Press.
- N. Le Roux and Y. Bengio (2008). Representational power of restricted Boltzmann machines and deep belief networks. *Neural computation* **20**, 1631–1649.

- F. Liang (2010). A double Metropolis–Hastings sampler for spatial models with intractable normalizing constants. *Journal of Statistical Computation and Simulation* **80**, 1007–1022.
- N. Meinshausen and P. Bühlmann (2006). High-dimensional graphs and variable selection with the Lasso. *The Annals of Statistics* **34**, 1436 – 1462.
- N. Meinshausen and P. Bühlmann (2010). Stability selection. *Journal of the Royal Statistical Society: Series B (Statistical Methodology)* **72**, 417–473.
- T. J. Mitchell and J. J. Beauchamp (1988). Bayesian variable selection in linear regression. *Journal of the American Statistical Association* **83**, 1023–1032.
- J. Møller, A. N. Pettitt, R. Reeves, and K. K. Berthelsen (2006). An efficient Markov chain Monte Carlo method for distributions with intractable normalising constants. *Biometrika* **93**, 451–458.
- G. Montufar and N. Ay (2011). Refinements of universal approximation results for deep belief networks and restricted Boltzmann machines. *Neural computation* **23**, 1306–1319.
- I. Murray, Z. Ghahramani, and D. MacKay (2012). MCMC for doubly-intractable distributions. *arXiv preprint arXiv:1206.6848* .
- R. M. Neal (2001). Annealed importance sampling. *Statistics and Computing* **11**, 125–139.
- R. M. Neal et al. (2011). MCMC using Hamiltonian dynamics. *Handbook of Markov chain Monte Carlo* **2**, 2.
- W. K. Newey (1991). Uniform convergence in probability and stochastic equicontinuity. *Econometrica: Journal of the Econometric Society* pages 1161–1167.
- N. Parikh and S. Boyd (2014). Proximal algorithms. *Foundations and trends[®] in Optimization* **1**, 127–239.
- T. Park and G. Casella (2008). The Bayesian lasso. *Journal of the American Statistical Association* **103**, 681–686.
- I. Pinelis (2020). Exact lower and upper bounds on the incomplete gamma function. *arXiv preprint arXiv:2005.06384* .

- R. B. Potts (1952). Some generalized order-disorder transformations. In *Mathematical proceedings of the cambridge philosophical society*, volume 48, pages 106–109. Cambridge University Press.
- A. P. Privitera, V. Barresi, and D. F. Condorelli (2021). Aberrations of chromosomes 1 and 16 in breast cancer: a framework for cooperation of transcriptionally dysregulated genes. *Cancers* **13**, 1585.
- C. R. Rao (1945). Information and accuracy attainable in the estimation of statistical parameters. kotz s & johnson nl (eds.), *breakthroughs in statistics volume i: Foundations and basic theory*, 235–248.
- P. Ravikumar, M. J. Wainwright, and J. D. Lafferty (2010). High-dimensional Ising model selection using ℓ_1 -regularized logistic regression. *The Annals of Statistics* **38**, 1287–1319.
- L. Roach and X. Gao (2023). Graphical local genetic algorithm for high-dimensional log-linear models. *Mathematics* **11**, 2514.
- A. J. Rothman, E. Levina, and J. Zhu (2010). Sparse multivariate regression with covariance estimation. *Journal of Computational and Graphical Statistics* **19**, 947–962.
- R. Salakhutdinov and G. Hinton (2009). Deep Boltzmann machines. In *Artificial intelligence and statistics*, pages 448–455. PMLR.
- R. Salakhutdinov, A. Mnih, and G. Hinton (2007). Restricted Boltzmann machines for collaborative filtering. In *Proceedings of the 24th international conference on Machine learning*, pages 791–798.
- R. Salakhutdinov and I. Murray (2008). On the quantitative analysis of deep belief networks. In *Proceedings of the 25th International Conference on Machine Learning*, pages 872–879.
- P. Smolensky (1986). Information processing in dynamical systems: Foundations of harmony theory. In *Parallel distributed processing: Explorations in the microstructure of cognition*, pages 194–281–. MIT Press, Cambridge, MA.
- J. Stoehr, A. Benson, and N. Friel (2019). Noisy Hamiltonian Monte Carlo for doubly intractable distributions. *Journal of Computational and Graphical Statistics* **28**, 220–232.

- I. Sutskever and T. Tieleman (2010). On the convergence properties of contrastive divergence. In *Proc. AISTATS*, pages 789–795.
- TCGA (2012). Comprehensive molecular portraits of human breast tumours. *Nature* **490**, 61–70.
- R. Tibshirani (1996). Regression shrinkage and selection via the lasso. *Journal of the Royal Statistical Society. Series B (Methodological)* **58**, 267–288.
- R. S. Varga (2010). *Gervogorin and his circles*, volume 36. Springer Science & Business Media.
- M. J. Wainwright and M. I. Jordan (2008). Graphical models, exponential families, and variational inference. *Foundations and Trends[®] in Machine Learning* **1**, 1–305.
- C. F. J. Wu (1983). On the Convergence Properties of the EM Algorithm. *The Annals of Statistics* **11**, 95 – 103.
- X. Xiao et al. (2022). Tmprss2 serves as a prognostic biomarker and correlated with immune infiltrates in breast invasive cancer and lung adenocarcinoma. *Frontiers in Molecular Biosciences* **9**, 647826.
- E. Yang, G. Allen, Z. Liu, and P. Ravikumar (2012). Graphical models via generalized linear models. In F. Pereira, C. Burges, L. Bottou, and K. Weinberger, editors, *Advances in Neural Information Processing Systems*, volume 25. Curran Associates, Inc.
- E. Yang, P. Ravikumar, G. I. Allen, and Z. Liu (2015). Graphical models via univariate exponential family distributions. *Journal of Machine Learning Research* **16**, 3813–3847.
- E. Yang, P. K. Ravikumar, G. I. Allen, and Z. Liu (2013). On Poisson graphical models. *Advances in neural information processing systems* **26**,.
- Y.-L. Yu (2013). On decomposing the proximal map. *Advances in neural information processing systems* **26**,.
- M. Yuan, A. Ekici, Z. Lu, and R. Monteiro (2007). Dimension reduction and coefficient estimation in multivariate linear regression. *Journal of the Royal Statistical Society: Series B (Statistical Methodology)* **69**, 329–346.
- S. Zhang, L. Yao, A. Sun, and Y. Tay (2019). Deep learning based recommender system: A survey and new perspectives. *ACM computing surveys (CSUR)* **52**, 1–38.

Supplementary Material to

Likelihood Based Inference in Fully and Partially Observed Exponential Family Graphical Models with Intractable Normalizing Constants

Table of Contents

S.1 Proofs	S.2
S.1.1 Proof of Proposition 3.2	S.2
S.1.2 Proof of Proposition 3.3	S.3
S.1.3 Auxiliary results for Theorems 6.4 and 6.5	S.3
S.1.4 Proof of Theorem 6.4	S.6
S.1.5 Proof of Theorem 6.5	S.9
S.1.6 Proof of Theorem 6.6	S.11
S.2 A Simple Accept–Reject Sampler for $p_{\theta}(\cdot)$	S.14
S.3 Algorithmic Details for Section 4	S.15
S.3.1 Tuning λ in (8) and model selection	S.15
S.3.2 HMC for PEGMs	S.16
S.4 Additional Numerical Experiments	S.18
S.4.1 Likelihood vs. pseudo-likelihood based CIs in low dimensions	S.18
S.4.2 A comparison of RBM and BM representational power	S.18
S.5 Additional Data Analysis Results	S.21
S.5.1 Additional results for movie ratings network	S.21
S.5.2 Additional results for breast cancer network	S.26

S.1 Proofs

S.1.1 Proof of Proposition 3.2

(a). (Proof for z_θ). For brevity, define $T_j = T_j(X_j)$ and $T_{jk} = T_{jk}(X_j, X_k)$. Recall $\phi = \text{diag}(\theta)$. Thus, from Equation (2), $q_\theta(X)/q_\phi(X) = \exp\left\{\sum_{(j,k) \in E} \theta_{jk} T_{jk}\right\}$. However, the model of Equation (2) is of the form $p_\eta(X) = \exp\{\eta T(X) + H(X) - A(\eta)\}$ with $T(X) = (T_j, T_{jk})$ as the sufficient statistic. That is, $T(X)$ is a $p \times p$ symmetric matrix with T_j as the j th diagonal entry and T_{jk} as the (j, k) th off-diagonal entry. The moment generating function of exponential family distribution satisfies $M_{T,\eta}(u) = \mathbb{E}_\eta(\exp(u^T T(X))) = \exp(A(u + \eta) - A(\eta))$. Setting $u = \theta - \text{diag}(\theta)$, and $\phi = \text{diag}(\theta)$, one has, $u + \phi = \theta \in \Theta$. Similarly, $\phi \in \Theta$, because this corresponds to the special case where the p variables are independent. Using the fact that for any valid parameter $\gamma \in \Theta$ we have $A(\gamma) < \infty$ in an exponential family model, shows that:

$$\mathbb{E}_\phi(q_\theta(X)/q_\phi(X)) = M_{T,\phi}(u) = \exp(A(u + \phi) - A(\phi)) = \exp(A(\theta) - A(\phi)) < \infty.$$

Similarly, if, $2u + \phi \in \Theta$, then, $\mathbb{E}_\phi\{(q_\theta(X)/q_\phi(X))^2\} = M_{T,\phi}(2u) = \exp(A(2u + \phi) - A(\phi)) < \infty$. Thus, $\text{Var}_\phi(q_\theta(X)/q_\phi(X)) < \infty$.

(b). (Proof for $\nabla_\theta z(\theta)$). Next consider $\nabla_\theta z(\theta)$. For $(j, k) \in E$, $\frac{\nabla_{\theta_{jk}} q_\theta(X)}{q_\phi(X)} = \frac{q_\theta(X)}{q_\phi(X)} T_{jk}$.

Thus,

$$\mathbb{E}_\phi \left\{ \left(\frac{\nabla_{\theta_{jk}} q_\theta(X)}{q_\phi(X)} \right)^2 \right\} = \mathbb{E}_\phi \left\{ \left(\frac{q_\theta(X)}{q_\phi(X)} \right)^2 T_{jk}^2 \right\} \leq \left\{ \mathbb{E}_\phi \left(\frac{q_\theta^{2a}(X)}{q_\phi^{2a}(X)} \right) \right\}^{1/a} [\mathbb{E}_\phi (T_{jk}^{2b})]^{1/b} < \infty,$$

where $a > 1$, $b > 1$, $(1/a + 1/b) = 1$ and the claim in the previous display is a consequence of the Hölder inequality. Similar to Part (a), and taking $a = 1 + \delta$, we have: $\mathbb{E}_\phi \left(\frac{q_\theta^{2a}(X)}{q_\phi^{2a}(X)} \right) = M_{T,\phi}(2au) = M_{T,\phi}(2(1 + \delta)u)$, which is bounded if $(2(1 + \delta)u + \phi) \in \Theta$, for some $\delta > 0$. The boundedness of $E_\phi (T_{jk}^{2b})$ follows from the fact that for an exponential family distribution, the sufficient statistic also belongs to an exponential family, for which moments of all orders

exist (Theorem 8.1, [Barndorff-Nielsen, 1978](#)). Repeating the calculation for all $(j, k) \in E$, the result follows. If $(j, k) \notin E$, the variance is zero and the result is trivial.

S.1.2 Proof of Proposition 3.3

Since $\phi = \text{diag}(\theta)$ and X is distributed according to a PEGM, we have $U = q_\theta(X)/q_\phi(X) = \exp\{\sum_{(j,k) \in E} \theta_{jk} X_j X_k\}$. Next, recall that a function $g : \mathbb{R}^p \rightarrow \mathbb{R}$ is said to have the bounded difference property if for some non-negative constants c_1, \dots, c_p ,

$$\sup_{x_1, \dots, x_p, x_{j'} \in \mathbb{R}^p} |g(x_1, \dots, x_j, \dots, x_p) - g(x_1, \dots, x_{j'}, \dots, x_p)| \leq c_j. \quad (\text{S.1})$$

In the current context, let $U = U(X_1, \dots, X_j, \dots, X_p)$ and $U' = U(X_1, \dots, X_{j'}, \dots, X_p)$. By assumption, each X_j has support in $[a_j, b_j]$. Without loss of generality, let $|b_j| \geq |a_j|$ for all $j = 1, \dots, p$. Clearly, $U \leq \exp\{\sum_{(j,k) \in E} \theta_{jk} |X_j X_k|\} \leq \exp\{\sum_{(j,k) \in E} \theta_{jk} |b_j b_k|\}$. Similarly, U' is also bounded. Then by the triangle inequality, $|U - U'| = |U| + |U'| \leq 2 \exp\{\sum_{(j,k) \in E} \theta_{jk} |b_j b_k|\}$. Thus, U is of bounded difference according to the definition (S.1). The second assertion then follows from [Boucheron et al. \(2003, Theorem 12\)](#). Noting that $V = X_j X_k U$, the same argument for V then applies.

S.1.3 Auxiliary results for Theorems 6.4 and 6.5

In this subsection, we record a few auxiliary results which will be used to prove Theorems in Section 6 of the main draft. The first result is an exponential concentration result, which is used to prove Theorem 6.4. The second result is needed for the proof of Theorem 6.5, and characterizes the prior Kullback-Leibler support set in terms of the Euclidean distance between the true parameter and prior realizations.

Proposition S.1.1. *Suppose we observe $X_1, \dots, X_n \stackrel{iid}{\sim} \text{PEGM}(\theta_0)$ where the model satisfies Assumption 2.2 and Assumption 2.3. Let $\mu_0 = (\mu_{0,jk})$ be the matrix of moments, i.e.*

$\mu_{0,jk} = \mathbb{E}_{\theta_0}[T(X_j, X_k)]$ when $j \neq k$, and $\mu_{0,jj} = \mathbb{E}_{\theta_0}[T(X_j)]$. Define $S_n = \sum_{i=1}^n T(X_{ij}, X_{ik})$.

Then for some $c \geq 0$

$$\mathbb{P}[|S_n - n\mu_{0,jk}| > n\nu] \leq 2 \exp(-cn\nu^2),$$

for $0 \leq \nu \leq \kappa_5$.

Proof. Define $S_n = \sum_{i=1}^n T(X_{ij}, X_{ik})$. We have for any s ,

$$\begin{aligned} \mathbb{P}(S_n - n\mu_{0,jk} > n\nu) &\leq \mathbb{E}[e^{s(S_n - n\mu_{0,jk})}]e^{-sn\nu} \\ &= \prod_{i=1}^n \mathbb{E}[e^{sT(X_{ij}, X_{ik})}]e^{-ns(\mu_{0,jk} + \nu)}. \end{aligned}$$

Write $T_j = T(X_j)$ and $T_{jk} = T(X_j, X_k)$. Then,

$$\begin{aligned} \log \mathbb{E}[\exp(\alpha T_{jk})] &= \log \int_{\mathcal{X}} \exp \left\{ \alpha T_{jk} + \sum_{j=1}^p \theta_{0j} T_j + \sum_{\substack{j,k=1 \\ j \neq k}}^p \theta_{0,jk} T_{jk} + \sum_{j=1}^p C(X_j) - A(\theta_0) \right\} dx \\ &= \bar{A}_{jk}(\theta_0; \alpha) - \bar{A}_{jk}(\theta_0; 0). \end{aligned}$$

Letting $\alpha \leq 1$ and using a Taylor expansion we get for some $\gamma \in (0, 1)$,

$$\begin{aligned} \bar{A}_{jk}(\theta_0; \alpha) - \bar{A}_{jk}(\theta_0; 0) &= \alpha \frac{\partial}{\partial \eta} \bar{A}_{jk}(\theta_0; \eta) \Big|_{\eta=0} + \frac{\alpha^2}{2} \frac{\partial^2}{\partial \eta^2} \bar{A}_{jk}(\theta_0; \eta) \Big|_{\eta=\gamma\alpha} \\ &\leq \alpha \kappa_3 + \frac{\alpha^2}{2} \kappa_5. \end{aligned}$$

Thus, $\mathbb{E}[\exp(sT_{jk})] \leq \exp(s\kappa_3 + \frac{s^2}{2}\kappa_5)$ for $s \leq 1$. Hence, for $0 \leq s \leq 1$, and then minimizing over s and since $\mu_{0,jk} \geq -\kappa_3$ we get,

$$\begin{aligned} \mathbb{P}(S_n - n\mu_{0,jk} > n\nu) &\leq e^{-ns\nu + ns^2 \frac{\kappa_5}{2}} \leq e^{-n \frac{\nu^2}{2\kappa_5}}, \quad \leq e^{-n \frac{(\nu + \mu_{0,jk} - \kappa_1)^2}{2\kappa_5}}, \quad s = (\nu + \mu_{0,jk} - \kappa_1) / \kappa_5 \\ &\leq e^{-cn\nu^2}, \quad \nu \leq (\kappa_1 + \kappa_3) / 2. \end{aligned}$$

when $\nu \leq \kappa_5$. Since $\mathbb{P}(|X| > t) \leq 2\mathbb{P}(X > t)$, the result follows. \square

A similar analysis leads to $\mathbb{P}(|S_n - \theta_{0,jj}| > n\nu) \leq 2 \exp(-cn\nu^2)$ for $0 \leq \nu \leq \kappa_4$.

For notational convenience, we write $\text{vech}(\theta) = \theta \in \mathbb{R}^{p(p+1)/2}$. Let $\mu \in \mathbb{R}^{p \times p}$ denote the corresponding symmetric matrix of mean parameters, i.e. $\mu_{jk} = \mathbb{E}[T(X_j, X_k)]$ for $j \neq k$ and $\mu_{jj} = \mathbb{E}[T(X_j)]$ for $j = 1, \dots, p$. Similarly, μ_0 is the mean matrix when the parameter is θ_0 . Again, we write $\text{vech}(\mu) = \mu$.

Proposition S.1.2. *Suppose π is some distribution on Θ . Then for every $\epsilon > 0$ there exists $\delta = \delta(\epsilon) > 0$ such that,*

$$\pi \{ \theta \in \Theta : KL(p_{\theta_0}, p_\theta) < \epsilon \} \geq \pi \{ \theta \in \Theta : \|\theta - \theta_0\|_2 < \delta \}.$$

Proof. It is straightforward to establish that $KL(p_{\theta_0}, p_\theta) = \langle \theta_0 - \theta, \mu_0 \rangle + \log z(\theta) - \log z(\theta_0)$. Indeed,

$$\begin{aligned} KL(p_{\theta_0}, p_\theta) &= \log z(\theta) - \log z(\theta_0) + \sum_j (\theta_{0,jj} - \theta_{jj}) \int T(x_j) p_{\theta_0}(x) dx \\ &\quad + \sum_{j \neq k} (\theta_{0,jk} - \theta_{jk}) \int T(x_j, x_k) p_{\theta_0}(x) \\ &= \langle \theta - \theta_0, \mu_0 \rangle. \end{aligned}$$

Write $A(\theta) = \log z(\theta)$ and $A(\theta_0) = \log z(\theta_0)$. It is well known that $A(\theta)$ is convex and has derivatives of all orders (Wainwright and Jordan, 2008, Proposition 3.1). Furthermore, $\nabla A(\theta) = \mu$ for all θ . Also, Taylor's theorem implies that for some $\gamma \in (0, 1)$,

$$\begin{aligned} A(\theta) &= A(\theta_0) + \langle \nabla A(\theta_0), \theta - \theta_0 \rangle + (\theta - \theta_0)^\top \left[\int_0^1 (1 - \gamma) \{ \nabla^2 A(\theta_0 + \gamma(\theta - \theta_0)) \} d\gamma \right] (\theta - \theta_0) \\ &\leq A(\theta_0) + \langle \nabla A(\theta_0), \theta - \theta_0 \rangle + (1 - \gamma) \|\theta - \theta_0\|_2^2 \lambda_{\max}[\nabla^2 A(\theta_0 + \gamma(\theta - \theta_0))], \end{aligned}$$

where $\lambda_{\max}(P)$ is the largest eigenvalue of a matrix P . Taking the limit $\gamma \rightarrow 0$ we obtain

$$\begin{aligned} KL(p_{\theta_0}, p_\theta) &= \langle \theta_0 - \theta, \mu_0 \rangle + A(\theta) - A(\theta_0) \\ &\leq \langle \theta_0 - \theta, \mu_0 \rangle + \langle -\nabla A(\theta_0), \theta_0 - \theta \rangle + \lambda_{\max}[\nabla^2 A(\theta_0)] \|\theta - \theta_0\|_2^2 \\ &= \lambda_{\max}[\nabla^2 A(\theta_0)] \|\theta - \theta_0\|_2^2. \end{aligned}$$

Hence $\{\theta : \|\theta - \theta_0\|_2 < \epsilon\} \subset \{\theta : \text{KL}(p_{\theta_0}, p_\theta) < \lambda_{\max}[\nabla^2 A(\theta_0)]\epsilon\}$ which implies that

$$\pi \{\theta \in \Theta : \text{KL}(p_{\theta_0}, p_\theta) < \lambda_{\max}[\nabla^2 A(\theta_0)]\delta\} \geq \pi \{\theta \in \Theta : \|\theta - \theta_0\|_2 < \delta\}.$$

□

S.1.4 Proof of Theorem 6.4

Define the matrix $S = (S_{jk})$ where $S_{jk} = \sum_{i=1}^n T(X_{ij}, X_{ik})$ if $j \neq k$ and $S_{jj} = \sum_{i=1}^n T(X_{ij})$.

Then $\ell(\theta) = \sum_{i=1}^n q_\theta(X_i) - nA(\theta) = \text{tr}(\theta S) - nA(\theta)$. The ℓ_1 -penalized estimator is defined as the minimizer of $-\ell(\theta) + \lambda \|\theta\|_1 = nA(\theta) - \text{tr}(\theta S) + \lambda \|\theta\|_1$. Let

$$\begin{aligned} Q(\theta) &= nA(\theta) - \text{tr}(\theta S) + \lambda \|\theta\|_1 - nA(\theta_0) + \text{tr}(\theta_0 S) - \lambda \|\theta_0\|_1 \\ &= n[A(\theta) - A(\theta_0)] - \text{tr}[(\theta - \theta_0)(S - \mu_0)] - \text{tr}[(\theta - \theta_0)\mu_0] + \lambda[\|\theta\|_1 - \|\theta_0\|_1]. \end{aligned}$$

Then, the ℓ_1 penalized estimate minimizes $Q(\theta)$. Define $\Delta = \theta - \theta_0$ and $G(\Delta) = Q(\theta_0 + \Delta)$. Equivalently, we want to minimize $G(\Delta)$ with respect to Δ . First, note that for any $\alpha \in (0, 1)$ and $\theta_1, \theta_2 \in \Theta$,

$$\begin{aligned} \alpha Q(\theta_1) &= n\alpha[A(\theta_1) - A(\theta_0)] - \text{tr}[\alpha(\theta_1 - \theta_0)(S - \mu_0)] - \text{tr}[\alpha(\theta_1 - \theta_0)\mu_0] \\ &\quad + \lambda\alpha[\|\theta_1\|_1 - \|\theta_0\|_1], \\ (1 - \alpha)Q(\theta_2) &= n(1 - \alpha)[A(\theta_2) - A(\theta_0)] - \text{tr}[(1 - \alpha)(\theta_2 - \theta_0)S] - \text{tr}[(1 - \alpha)(\theta_2 - \theta_0)\mu_0] \\ &\quad + \lambda(1 - \alpha)[\|\theta_1\|_1 - \|\theta_0\|_1]. \end{aligned}$$

This implies that if $\theta^* = \alpha\theta_1 + (1 - \alpha)\theta_2$ then,

$$\begin{aligned} \alpha Q(\theta_1) + (1 - \alpha)Q(\theta_2) &\geq n[A(\theta^*) - A(\theta_0)] - \text{tr}(\theta^* S) - \text{tr}(\theta^* \mu_0) + \lambda[\|\theta^*\|_1 - \|\theta_0\|_1] \\ &= Q(\theta^*), \end{aligned}$$

by triangle inequality and since $A(\theta)$ is convex. Similarly, if $\Delta_1 = \theta_1 - \theta_0$ and $\Delta_2 = \theta_2 - \theta_0$, then $\alpha G(\Delta_1) + (1 - \alpha)G(\Delta_2) \geq G(\Delta^*)$ where $\Delta^* = \theta^* - \theta_0$. Thus, $G(\Delta)$ is convex and $G(0) = 0$. Hence, if $\hat{\Delta} = \inf_{\Delta} G(\Delta)$, then $G(\hat{\Delta}) \leq 0$.

Now, $G(\Delta) = n[A(\theta_0 + \Delta) - A(\theta_0)] - \text{tr}[\Delta(S - \mu_0)] - \text{tr}(\Delta\mu_0) + \lambda[\|\theta_0 + \Delta\|_1 - \|\theta_0\|_1]$.

A Taylor expansion of $A(\theta_0 + \Delta) - A(\theta_0)$ yields

$$A(\theta_0 + \Delta) - A(\theta_0) = \text{tr}(\nabla A(\theta_0)\Delta) + \tilde{\Delta}^\top \left[\int_0^1 (1-v) \frac{\partial^2}{\partial v^2} A(\theta_0 + v\Delta) dv \right] \tilde{\Delta},$$

where $\tilde{\Delta} = \text{vec}(\Delta)$. Thus $G(\Delta) = \tilde{\Delta}^\top \left[\int_0^1 (1-v) \partial^2 A(\theta_0 + v\Delta) dv \right] \tilde{\Delta} - \text{tr}[\Delta(S - \mu_0)] + \lambda[\|\theta_0 + \Delta\|_1 - \|\theta_0\|_1]$. That is, $G(\Delta) = T_1 - T_2 + T_3$. Let $\mathbf{S} = \{j \leq k : \theta_{0,jk} \neq 0, j, k = 1, \dots, p\}$. We next work with each term separately. We have

$$\begin{aligned} |T_2| = |\text{tr}[\Delta(S - \mu_0)]| &\leq \left| \sum_{j \leq k} \sum (s_{jk} - \mu_{0,jk}) \Delta_{jk} \right| \\ &\leq \left| \sum_{j \leq k: \theta_{0,jk} = 0} \sum (s_{jk} - \mu_{0,jk}) \Delta_{jk} \right| + \left| \sum_{j \leq k: \theta_{0,jk} \neq 0} \sum (s_{jk} - \mu_{0,jk}) \Delta_{jk} \right| \\ &\leq \max_{\mathbf{S}^c} |s_{jk} - \mu_{0,jk}| \|\Delta_{\mathbf{S}^c}\|_1 + \sqrt{s} \max_{\mathbf{S}} |s_{jk} - \mu_{0,jk}| \|\Delta_{\mathbf{S}}\|_F, \end{aligned}$$

where the second bound comes from Cauchy-Schwarz inequality. From Proposition S.1.1, and the union bound we have that with probability at least $1 - 2e^{-C \log p/n^2}$, $\max_{j \leq k} |s_{jk} - \mu_{0,jk}| \leq C_1 \sqrt{\log p/n}$ for some $C, C_1 > 0$. Thus we have with probability tending to 1,

$$|T_2| \leq C_1 \sqrt{\frac{\log p}{n}} \|\Delta_{\mathbf{S}^c}\|_1 + C_1 \sqrt{\frac{s \log p}{n}} \|\Delta_{\mathbf{S}}\|_F.$$

Next, we work with $T_3 = \lambda[\|\theta_0 + \Delta\|_1 - \|\theta_0\|_1]$. Clearly, $\|\theta_0\|_1 = \|\theta_{0\mathbf{S}}\|_1$ and $\|\theta_0 + \Delta\|_1 = \|\theta_{0\mathbf{S}} + \Delta_{\mathbf{S}}\|_1 + \|\Delta_{\mathbf{S}^c}\|_1$. Thus, by triangle inequality

$$T_3 \geq \lambda(\|\Delta_{\mathbf{S}^c}\|_1 - \|\Delta_{\mathbf{S}}\|_1).$$

Set $\lambda = \frac{C_1}{\epsilon} \sqrt{\frac{\log p}{n}}$ for some $\epsilon > 0$. Then since $\|\Delta_{\mathbf{S}}\|_1 \leq \sqrt{s} \|\Delta_{\mathbf{S}}\|_F$, we have,

$$\begin{aligned} T_3 &\geq \frac{C_1}{\epsilon} \sqrt{\frac{\log p}{n}} \|\Delta_{\mathbf{S}^c}\|_1 - \frac{C_1}{\epsilon} \sqrt{\frac{s \log p}{n}} \|\Delta_{\mathbf{S}}\|_F \\ &\geq \frac{C_1}{\epsilon} \sqrt{\frac{\log p}{n}} \|\Delta_{\mathbf{S}^c}\|_1 - \frac{C_1}{\epsilon} \sqrt{\frac{s \log p}{n}} \|\Delta\|_F. \end{aligned}$$

Finally, for T_1 we have for $\Delta \in \Theta_n(M) = \{\Delta : \Delta = \Delta^T, \|\Delta\|_F = Mr_n\}$,

$$\begin{aligned} T_1 &= \tilde{\Delta}^T \left[\int_0^1 (1-v) \frac{\partial^2}{\partial v^2} A(\theta_0 + v\Delta) dv \right] \tilde{\Delta} \\ &\geq \lambda_{\min} \left(\int_0^1 (1-v) \frac{\partial^2}{\partial v^2} A(\theta_0 + v\Delta) dv \right) \|\Delta\|_F^2 \\ &\geq \|\Delta\|_F^2 \int_0^1 (1-v) \lambda_{\min} \left(\frac{\partial^2}{\partial v^2} A(\theta_0 + v\Delta) \right) dv \\ &\geq \|\Delta\|_F^2 \min_{0 \leq v \leq 1} \lambda_{\min} \left(\frac{\partial^2}{\partial v^2} A(\theta_0 + v\Delta) \right) \int_0^1 (1-v) dv \\ &\geq \frac{1}{2} \|\Delta\|_F^2 \min \left[\lambda_{\min} \left(\frac{\partial^2}{\partial \theta^2} A(\theta_0 + \bar{\Delta}) \right) : \|\bar{\Delta}\|_F \leq Mr_n \right] \\ &\geq \frac{1}{2} \|\Delta\|_F^2 \min \left[\lambda_{\min} \left(\frac{\partial^2}{\partial \theta^2} A(\theta_0) + \rho \|\bar{\Delta}\|_F : \|\bar{\Delta}\|_F \leq Mr_n \right) \right], \end{aligned}$$

where the last inequality follows from a Taylor expansion on $\frac{\partial^2}{\partial \theta^2} A(\theta_0)$ and Assumption 6.2.

Since $\|\bar{\Delta}\|_F \leq Mr_n$ and $Mr_n \rightarrow 0$ as $n \rightarrow \infty$ we have that,

$$\lambda_{\min} \left(\frac{\partial^2}{\partial \theta^2} A(\theta_0) + \rho \|\bar{\Delta}\|_F : \|\bar{\Delta}\|_F \leq Mr_n \right) \geq \frac{\beta}{2}.$$

Putting all the pieces together we obtain,

$$\begin{aligned} G(\Delta) &\geq \frac{n\beta}{4} \|\Delta\|_F^2 - C_1 \sqrt{\frac{\log p}{n}} \|\Delta_{\mathbf{S}^c}\|_1 \left(1 - \frac{1}{\epsilon}\right) - C_1 \sqrt{\frac{s \log p}{n}} \|\Delta_{\mathbf{S}}\|_F \left(1 + \frac{1}{\epsilon}\right) \\ &> 0, \end{aligned}$$

for sufficiently large M and n . Hence, we have argued that if $\hat{\Delta}$ is the minimizer of $G(\Delta)$ then $G(\hat{\Delta}) \leq 0$ and $\inf\{G(\Delta) : \Delta \in \Theta_n(M)\} > 0$, then $\hat{\Delta}$ must be inside the ball $\Theta_n(M)$, i.e. $\|\hat{\Delta}\|_F \leq Mr_n$.

S.1.5 Proof of Theorem 6.5

The vectorized data generating parameter $\text{vech}(\theta_0) \in \Theta \subset \mathbb{R}^{p(p+1)/2}$. By Assumption 6.2, Θ is open, hence there exists $\epsilon > 0$ such that $\{\theta : \|\theta - \theta_0\|_2 < \epsilon\} \subset \Theta$. Moreover, from Proposition S.1.2, we have

$$\pi \{\theta \in \Theta : \|\theta - \theta_0\|_2 < \epsilon\} \geq \pi \{\theta \in \Theta : \text{KL}(p_{\theta_0}, p_\theta) < \delta(\epsilon)\}.$$

Hence, if we can show that $\pi \{\theta : \|\theta - \theta_0\|_2 < \epsilon\} > 0$ for every sufficiently small $\epsilon > 0$, then that would imply posterior consistency in weak topology (Ghosal and Van der Vaart, 2017, Example 6.20). To that end, we have

$$\begin{aligned} \pi \{\theta : \|\theta - \theta_0\|_2 < \epsilon\} &\geq \frac{\pi_L \{\theta : \|\theta - \theta_0\|_2 < \epsilon\}}{\pi_L(\Theta)} \\ &\geq \pi_L \{\theta : \|\theta - \theta_0\|_2 < \epsilon\} \end{aligned} \tag{S.2}$$

since $\pi_L(\Theta) \leq 1$, and where $\pi(\theta) \propto \pi_L(\theta)\mathbb{I}_{\theta \in \Theta}$. Next, we obtain a lower bound of $\pi_L \{\theta : \|\theta - \theta_0\|_2 < \epsilon\}$. To simplify notation, we show for $\theta, \theta_0 \in \mathbb{R}^p$, and θ_0 having s non-zero entries

$$\pi_L \{\theta : \|\theta - \theta_0\|_2 < \epsilon\} > 0.$$

The result then applies to our context where $\theta_0, \theta \in \mathbb{R}^{p(p+1)/2}$.

Define $S = \{j : |\theta_{0j}| \neq 0\}$. We then have

$$\begin{aligned} \mathbb{P}[\|\theta - \theta_0\|_2 < \delta] &\geq \mathbb{P}\left[\|\theta_S - \theta_{0S}\|_2 < \frac{\delta}{2}\right] \mathbb{P}\left[\|\theta_{S^c}\|_2 < \frac{\delta}{2}\right] \\ &\geq \prod_{j \in S} \mathbb{P}\left[|\theta_j - \theta_{0j}| < \frac{\delta}{2\sqrt{s}}\right] \int_{I_\lambda} \mathbb{P}\left[\|\theta_{S^c}\|_2 < \frac{\delta}{2} \mid \lambda \in I_\lambda\right] \pi(\lambda) d\lambda, \end{aligned}$$

where $I_\lambda = [\lambda_1, \lambda_2]$ with $\lambda_1 = \sqrt{\frac{np \log p}{s}}$ and $\lambda_2 = 2\lambda_1$. We next focus on the conditional probability:

$$\mathbb{P}\left[\|\theta_{0S^c}\|_2 \leq \frac{\delta}{2} \mid \lambda \in I_\lambda\right] \geq \prod_{j \notin S} \mathbb{P}\left[|\theta_j| < \frac{\delta}{2\sqrt{p}} \mid \lambda \in I_\lambda\right].$$

First, we handle the term $\mathbb{P}\left[|\theta_j| < \frac{\delta}{2\sqrt{p}} \mid \lambda \in I_\lambda\right]$. Recall, if the random variable X is sub-exponential distribution with parameters (ν^2, ρ) , then,

$$\mathbb{P}[|X - \mu| \geq t] \leq \begin{cases} 2e^{-\frac{t^2}{2\nu^2}}, & \text{if } 0 < t \leq \frac{\nu^2}{\rho}, \\ 2e^{-\frac{t}{2\rho}}, & \text{if } t > \frac{\nu^2}{\rho}. \end{cases} \quad (\text{S.3})$$

Here $\theta_j \mid \lambda \sim \text{Laplace}(1/\lambda)$, and the Laplace distribution is sub-exponential with $\nu = 2/\lambda$ and $\rho = 2/\lambda$. Set $t = \frac{\delta}{2\sqrt{p}} = \frac{1}{2}\sqrt{\frac{s \log p}{np}}$ in (S.3) and note that $\nu^2/\rho = 2/\lambda$. Thus, for any $\lambda > 4\sqrt{\frac{np}{s \log p}}$ we have:

$$\mathbb{P}\left[|\theta_j| < \frac{\delta}{2\sqrt{p}} \mid \lambda\right] \geq 1 - 2e^{-\frac{\delta\lambda}{4\sqrt{p}}}.$$

Specifically, for any $\lambda \in I_\lambda$ we get,

$$\mathbb{P}\left[|\theta_j| < \frac{\delta}{2\sqrt{p}} \mid \lambda \in I_\lambda\right] \geq 1 - 2e^{-\frac{\delta\lambda}{4\sqrt{p}}} \geq 1 - 2e^{\frac{\delta\lambda_1}{4\sqrt{p}}} = 1 - 2e^{-\frac{1}{4}\log p}.$$

Thus for some $C > 0$, $\mathbb{P}\left[|\theta_j| < \frac{\delta}{2\sqrt{p}} \mid \lambda\right] \geq e^{-C \log p}$ for some $C > 0$. We also have that $\mathbb{P}[\lambda \in I_\lambda] = \mathbb{P}[\lambda > \lambda_1] - \mathbb{P}[\lambda > \lambda_2]$. Next, we record the following upper and lower bounds for the incomplete Gamma function (Pinelis, 2020),

$$\frac{x^a e^{-x}(x - a - 1)}{(x - a)^2 + a} \leq \Gamma(a, x) = \int_x^\infty t^{a-1} e^{-t} dt \leq \frac{x^a e^{-x}}{x - a}.$$

Also, we have $(a/e)^{a-1} \leq \Gamma(a) \leq (a/2)^{a-1}$. Set $\alpha = a_\lambda$ and $\beta = b_\lambda$. Thus,

$$\begin{aligned} \mathbb{P}(\lambda \in I_\lambda) &= \frac{\beta^\alpha}{\Gamma(\alpha)} \Gamma(\alpha, \beta\lambda_1) - \frac{\beta^\alpha}{\Gamma(\alpha)} \Gamma(\alpha, 2\beta\lambda_1) \\ &= e^{\log \beta} e^{-(\alpha-1)\log \alpha} e^{(\alpha-1)\log 2} \Gamma(\alpha, \beta\lambda_1) - e^{\log \beta} e^{-(\alpha-1)\log \alpha} e^{(\alpha-1)\log 2} \Gamma(\alpha, 2\beta\lambda_1) \\ &\geq e^{\log \beta} e^{-(\alpha-1)\log \alpha} e^{K(\alpha-1)} (\beta\lambda_1)^\alpha e^{-C\beta\lambda_1}, \quad \text{for } \alpha = O(\beta\lambda_1) \\ &= e^{\log \beta} e^{-(\alpha-1)\log \alpha} e^{(\alpha-1)\log 2} e^{\alpha \log \beta \lambda_1} e^{-C\beta\lambda_1} \\ &\geq e^{-C\beta\lambda_1} \geq e^{-Cs \log p}, \end{aligned}$$

for $\beta = O\left(s\sqrt{\frac{s \log p}{np}}\right)$. Hence, we have that,

$$\int_{I_\lambda} \mathbb{P}\left[\|\theta_{S^c}\|_2 < \frac{\delta}{2} \mid \lambda \in I_\lambda\right] \pi(\lambda) d\lambda \geq e^{-Cs \log p},$$

for some $C > 0$. We now handle the term $\mathbb{P}[|\theta_j - \theta_{0j}| < \frac{\delta}{2\sqrt{s}}]$. Since $\lambda \sim \text{Gamma}(\alpha, \beta)$, marginal density of θ_j is:

$$f(\theta_j) = \frac{\beta^\alpha}{2\Gamma(\alpha)} \frac{\Gamma(\alpha + 1)}{(|\theta_j| + \beta)^\alpha} = \frac{(\alpha + 1)\beta^\alpha}{2(|\theta_j| + \beta)^\alpha}.$$

Let $A = \{\theta_j : |\theta_j - \theta_{0j}| \leq \delta^*, j \in S\}$ where $\delta^* = \frac{\delta}{2\sqrt{s}}$. We have for α, β as chosen above

$$\begin{aligned} \mathbb{P}[\theta_j \in A] &= \int_A \frac{(\alpha + 1)\beta^\alpha}{2(|\theta_j| + \beta)^\alpha} d\theta_j \\ &\geq e^{-\log 2} e^{\alpha \log \beta} e^{\log(\alpha+1)} e^{\log \delta^*} e^{-\alpha(|\theta_{0j}| + \delta^* + \beta)} \\ &\geq e^{-C\alpha \log(\frac{1}{\beta})}, \end{aligned}$$

which establishes that $\pi_L\{\theta : \|\theta - \theta_0\|_2 < \epsilon\} > 0$. Hence, the theorem follows.

S.1.6 Proof of Theorem 6.6

For simplicity, consider one observed sample, i.e. $n = 1$. The same arguments apply for a general sample size. The complete data log-likelihood is:

$$\log p_\theta(\mathbf{v}, \mathbf{h}) = \sum_{j=1}^p \theta_{jj} v_j + \sum_{k=p+1}^{p+m} \theta_{kk} h_k + \sum_{j=1}^p \sum_{k=p+1}^{p+m} \theta_{jk} v_j h_k - \log z(\theta).$$

Given the current iteration $\theta^{(t)}$, let,

$$\begin{aligned} Q(\theta; \theta^{(t)}) &= \mathbb{E}_{\theta^{(t)}}[\ell_c(\theta)] \\ &= \sum_{j=1}^p \theta_{jj} v_j + \sum_{k=p+1}^{p+m} \theta_{kk} \mathbb{E}_{\theta^{(t)}}[h_k \mid \mathbf{v}] + \sum_{j=1}^p \sum_{k=p+1}^{p+m} \theta_{jk} v_j \mathbb{E}_{\theta^{(t)}}[h_k \mid \mathbf{v}] - \log z(\theta) \\ &= g(\mathbf{v}; \theta, \theta^{(t)}) - \log z(\theta), \end{aligned}$$

where $\mathbb{E}_{\theta^{(t)}}[h_k \mid \mathbf{v}] = \mathbb{P}_{\theta^{(t)}}[h_k \mid \mathbf{v}] = \sigma(\theta_{kk}^{(t)} + \sum_{j=1}^p \theta_{jk}^{(t)} v_j)$, and $g(\mathbf{v}; \theta, \theta^{(t)}) = Q(\theta; \theta^{(t)}) - \log z(\theta)$. Then the update (9), is obtained by setting $\frac{\partial Q(\theta; \theta^{(t)})}{\partial \theta} = 0$. Also, there exists a suitable step size γ such that $\theta^{(t+1)}$ will satisfy $Q(\theta^{(t+1)}; \theta^{(t)}) \geq Q(\theta^{(t)}; \theta^{(t)})$. Furthermore, $Q(\theta_1; \theta_2)$ is continuous for all θ_1 and θ_2 . Then from (Wu, 1983, Theorem 2) any generalized EM sequence $\theta^{(t)}$ converges to a stationary point of $\log p_{\theta}(\mathbf{v})$.

Consider any such sequence with starting value $\theta^{(0)}$. In what follows, we write $\|M\|_2$ to be the Euclidean norm of a symmetric matrix M , i.e. $\|M\|_F = \|\text{vech}(M)\|_2$. Let $\theta^{(t)}$ and $\theta_{\star}^{(t)}$ denote the sequences obtained by an exact EM algorithm and a Monte Carlo EM algorithm (which is our case). Then the EM and the Monte Carlo EM are of the following form:

$$\begin{aligned}\theta^{(t+1)} &= \theta^{(t)} + \gamma_t \nabla Q(\theta^{(t)}; \theta^{(t)}), \\ \theta_{\star}^{(t+1)} &= \theta^{(t)} + \gamma_t \nabla Q^{\star}(\theta_{\star}^{(t)}; \theta_{\star}^{(t)}),\end{aligned}$$

where $\nabla Q^{\star}(\theta; \psi)$ is the Monte Carlo estimate of $\nabla Q(\theta; \psi)$ for any $\theta, \psi \in \Theta$. Let $T_N^{(1)}(\theta)$ and $T_N^{(2)}(\theta)$ denote the Monte Carlo estimates of $\log z(\theta)$ and $\nabla \log z(\theta)$, respectively. Clearly, $T_N^{(1)}(\theta)$ converges to $\log z(\theta)$, pointwise and almost surely. That this is true for $T_N^{(2)}(\theta)$ as an estimator of $\nabla \log z(\theta)$ follows from the continuous mapping theorem. Hence, we have,

$$\begin{aligned}\|\theta^{(1)} - \theta_{\star}^{(1)}\|_2 &= \|\gamma_1 \nabla Q(\theta^{(0)}; \theta^{(0)}) - \gamma_1 Q^{\star}(\theta^{(0)}; \theta^{(0)})\|_2 \\ &\leq \gamma_1 \left\| \nabla \log z(\theta^{(0)}) - T_N^{(2)}(\theta^{(0)}) \right\|_2 \\ &\leq \gamma_1 \sup_{\theta \in \Theta} \left\| \nabla \log z(\theta) - T_N^{(2)}(\theta) \right\|_2 \leq \gamma_1 \epsilon,\end{aligned}$$

where taking supremum is possible as the convergence is uniform as we shall prove later.

More generally, if $\left\| \theta^{(t)} - \theta_{\star}^{(t)} \right\|_2 \leq \delta$, for some $\delta > 0$, then,

$$\begin{aligned}\|\theta^{(t+1)} - \theta_{\star}^{(t+1)}\|_2 &\leq \|\theta^{(t)} - \theta_{\star}^{(t)}\|_2 + \|\gamma_t \nabla Q(\theta^{(t)}; \theta^{(t)}) - \gamma_t \nabla Q^{\star}(\theta_{\star}^{(t)}; \theta_{\star}^{(t)})\|_2 \\ &\leq \delta + \gamma_t \left\| \nabla g(\mathbf{v}; \theta, \theta^{(t)}) - \nabla g(\mathbf{v}; \theta, \theta_{\star}^{(t)}) \right\|_2 + \gamma_t \left\| \nabla \log z(\theta^{(t)}) - T_N^{(2)}(\theta_{\star}^{(t)}) \right\|_2\end{aligned}$$

$$\begin{aligned}
&\leq \delta + \gamma_t \lambda_{\max}[\nabla^2 g(\mathbf{v}; \theta, \tilde{\theta}_1)] \|\theta^{(t)} - \theta_\star^{(t)}\|_2 + \gamma_t \left\| \nabla \log z(\theta^{(t)}) - T_N^{(2)}(\theta_\star^{(t)}) \right\|_2 \\
&\leq \delta + \gamma_t C_1 \delta + \gamma_t \left\| \nabla \log z(\theta^{(t)}) - \nabla \log z(\theta_\star^{(t)}) \right\|_2 + \gamma_t \left\| \nabla \log z(\theta_\star^{(t)}) - T_N^{(2)}(\theta_\star^{(t)}) \right\|_2 \\
&\leq \delta + \gamma_t C_1 \delta + \gamma_t \lambda_{\max}[\nabla^2 \log z(\tilde{\theta}_2)] + \gamma_t \epsilon \\
&\leq \delta + \gamma_t C_1 \delta + \gamma_t C_2 \delta + \gamma_t \epsilon \leq C \delta \gamma_t,
\end{aligned}$$

where $\tilde{\theta}_i = \theta^{(t)} + \rho_i(\theta^{(1)} - \theta_\star^{(t)})$ for $\rho_i \in (0, 1)$, and $i = 1, 2$. That the Hessian of $g(\mathbf{v}; \theta, \phi)$ is bounded by a global constant follows from the fact that $\nabla^2 g(\mathbf{v}; \theta, \phi)$ is continuous on the compact support of ϕ , and \mathbf{v} is bounded from the Gershgorin circle theorem (Varga, 2010). Similarly, the Hessian of $\log z(\theta)$ is also bounded on the compact support of θ . Hence, if $C\gamma_t \leq 1$, for all $t \geq 1$, then,

$$\sum_{t=1}^{\infty} \|\theta^{(t)} - \theta_\star^{(t)}\|_2 \leq \epsilon \sum_{t=1}^{\infty} \gamma_t = 0.$$

In other words, for sufficiently large t ,

$$\|\theta^{(t)} - \theta_\star^{(t)}\|_2 = O\left(\frac{1}{t^{1+\eta}}\right),$$

for some $\eta > 0$. It then remains to show that the convergence of $T_N^{(2)}(\theta)$ to $\nabla \log z(\theta)$ is uniform over Θ . Observe that:

$$T_N^{(2)}(\theta) = \frac{\sum_{i=1}^N \frac{\nabla q_\theta(Y_i)}{q_\phi(Y_i)}}{\sum_{i=1}^N \frac{q_\theta(Y_i)}{q_\phi(Y_i)}} = \frac{\sum_{i=1}^N D_1(Y_i; \theta)}{\sum_{i=1}^N D_2(Y_i; \theta)}, \quad (\text{say})$$

where $Y_i \in \{0, 1\}^{p+m}$ and $\phi = \text{diag}(\theta)$. Then,

$$\nabla T_N^{(2)}(\theta) = \frac{\sum_{i=1}^N \nabla D_1(Y_i; \theta)}{\sum_{i=1}^N D_2(Y_i; \theta)} - \frac{\sum_{i=1}^N D_1(Y_i; \theta)}{\left(\sum_{i=1}^N D_2(Y_i; \theta)\right)^2} \sum_{i=1}^N \nabla D_2(Y_i; \theta).$$

Therefore,

$$\begin{aligned} \left\| \nabla T_N^{(2)}(\theta) \right\|_2 &\leq \frac{1}{\left[\sum_{i=1}^N D_2(Y_i; \theta) \right]^{1/2}} \left\| \sum_{i=1}^N \nabla D_1(Y_i; \theta) \right\|_2 + \left[\frac{\sum_{i=1}^N D_1(Y_i; \theta)}{\left(\sum_{i=1}^N D_2(Y_i; \theta) \right)^2} \right]^{1/2} \left\| \sum_{i=1}^N \nabla D_2(Y_i; \theta) \right\|_2 \\ &\leq C, \end{aligned}$$

for some $C > 0$, due to the fact that $D_1, D_2, \nabla D_1, \nabla D_2$ are all continuous with respect to θ and Y_i is a bounded random variable, and since Θ is compact. Since by definition Θ is also convex, and $T_N^{(2)}(\theta)$ is infinitely differentiable, uniform convergence follows from (Newey, 1991, Corollary 2.2).

S.2 A Simple Accept–Reject Sampler for $p_\theta(\cdot)$

Generating samples from a Boltzmann distribution, of which PEGMs are special cases, remains a challenge; especially without resorting to computationally expensive MCMC techniques. However, our approach also accomplishes this goal. Specifically, for a given θ , suppose we simulate $Y \sim p_\phi(\cdot)$, where $\phi = \text{diag}(\theta)$. This is cheap, and does not require MCMC. Moreover, $z(\phi)$ is analytically available. Next, recall, $p_\theta(x) = q_\theta(x)/z(\theta)$. Thus, an accept–reject sampler for $p_\theta(\cdot)$ consists of the following two steps:

1. Simulate $Y \sim p_\phi(\cdot)$
2. Accept Y with probability $r = q_\theta(Y)/\{Mp_\phi(Y)\}$ where M is such that $q_\theta(Y) < Mp_\phi(Y)$ for all Y .

Thus, M must be chosen to satisfy the criterion:

$$\begin{aligned} \exp \left(\sum_j \theta_j Y_j + \sum_{j \neq k} \theta_{jk} Y_j Y_k \right) &< M \exp \left(\sum_j \theta_j Y_j \right) / z(\phi), \\ \text{i.e., } \exp \left(\sum_{j \neq k} \theta_{jk} Y_j Y_k \right) &< M z(\phi)^{-1}. \end{aligned}$$

However, a simple choice of M is available for several PEGMs. For example, in a Poisson graphical model, all off-diagonal elements of a valid θ are negative, and one may take $Mz(\phi)^{-1} = 1$, i.e., $M = z(\phi)$. Similarly, for Ising, where $Y_j = \{0, 1\}$ for all j , a simple choice is $\{M : Mz(\phi)^{-1} > \exp(p^2 \max_{jk} \theta_{jk})\}$. Other, less obvious choices of M may result in better average acceptance probabilities. We do not explore the details in this work.

S.3 Algorithmic Details for Section 4

S.3.1 Tuning λ in (8) and model selection

Here we describe how the value of the tuning parameter λ is selected in (8). Generally, pseudo-likelihood methods have a regression structure in that the likelihood of $X_j | X_{-j}$ is a generalized linear model for PEGMs. As a result, out-of-sample prediction is typically used for tuning parameter selection. This is, however, not the case when a full-likelihood analysis is implemented. In our work, we instead consider the out-of-sample log-likelihood to select the value of λ given estimated $\hat{\theta}_\lambda$ is available for a grid of values of λ : $[\lambda_l, \lambda_u]$. Specifically, we divide the observed data randomly into K -folds, of which $K - 1$ folds are used to obtain $\hat{\theta}_\lambda$ for each value of λ . The log-likelihood $\ell(\hat{\theta}_\lambda)$ is computed on the remaining fold. The process is repeated for each fold, and we choose $\hat{\theta}_\lambda$ to be our estimator for which we obtain the maximum out-of-sample log-likelihood. This generally results in improved Frobenius norm estimates of θ as reported in Table 1. However, it is well known that cross-validated estimates in penalized estimation procedures may provide sub-optimal performance in terms of model selection (Bühlmann and Van De Geer, 2011). To address this, we construct an estimator of θ that selects edges between nodes which are most often selected. Suppose, for R choices of λ , we obtain estimates $\hat{\mathbf{S}}_{\lambda_r} = \{(j, k) : \hat{\theta}_{\lambda_r, jk} \neq 0\}$.

Define $I_{jk}^r = \mathbb{I}\{(j, k) \in \hat{\mathbf{S}}_{\lambda_r}\}$. Then, we estimate the structure of the graph G by:

$$\hat{\mathbf{S}} = \left\{ (j, k) : \frac{1}{R} \sum_{r=1}^R I_{jk}^r > \pi_{thr}, \right\} \quad (\text{S.4})$$

where $0 < \pi_{thr} < 1$. The procedure closely resembles stability selection (Meinshausen and Bühlmann, 2010), except here we do not perform subsampling. Our experiments with and without subsampling resulted in similar performance. Hence, we omit that step. For the threshold π_{thr} , we use 0.6. Results from this choice are reported under the MCC column in Table 1. For fair comparison, we also implemented this structure learning method with pseudo-likelihood based approaches.

S.3.2 HMC for PEGMs

Suppose we observe iid data $\mathbf{X} = (X_{1\bullet}, \dots, X_{n\bullet})$ from some PEGM(θ). Consider the following prior structure over θ : $\pi(\theta) = \int \left[\prod_{j \leq k} \pi(\theta_{jk} | \tau) \right] g(\tau) d\tau$, i.e. the elements θ_{jk} are conditionally independent given a global shrinkage parameter τ . The posterior is then:

$$\pi(\theta | \mathbf{X}) \propto \left[\prod_{i=1}^n \frac{q_{\theta}(X_{i\bullet})}{z(\theta)} \right] \pi(\theta). \quad (\text{S.5})$$

We make two simplifying assumptions. First, we fix $\tau = 1$, noting that our procedure can be easily incorporated in the general case when $\tau \sim g$ with an additional layer of sampling. Second, we assume that the convexity of Θ can be represented as $C(\theta) \geq 0$ for a suitable choice of a differentiable $C(\theta)$.

Suppose $\pi(\theta_{jk})$ admits the marginal representation $\pi(\theta_{jk}) = \int \pi(\theta_{jk} | \rho_{jk}) \pi(\rho_{jk}) d\rho_{jk}$, with respect to some latent variables ρ_{jk} , and $\pi(\theta_{jk} | \rho_{jk})$ is differentiable. This is indeed the case for any prior that is a scale mixture of Gaussian. Then samples from the augmented posterior $\pi(\theta, \{\rho_{jk}\}_{j \leq k} | \mathbf{X})$ can be obtained by employing a Gibbs sampler that iterates between sampling from $\pi(\theta | \{\rho_{jk}\}_{j \leq k}, \mathbf{X})$ and $\pi(\{\rho_{jk}\}_{j \leq k} | \theta, \mathbf{X})$. We use a HMC sampler to sample from $\pi(\theta | \{\rho_{jk}\}_{j \leq k}, \mathbf{X})$ and sample ρ_{jk} 's in a block since these are conditionally

Algorithm S.1 Constrained HMC sampler for updating $\theta \mid \{\rho_{jk}\}_{j \leq k}, \mathbf{X}$

Input: θ [current state], ϵ [step size], L [number of leapfrog steps]**Output:** θ [next update]Sample $p \sim N(0, I)$ and set $p = p - \frac{1}{2}\epsilon \nabla_{\theta} U(\theta)$,**while** $l \leq L$ **do** $\theta = \theta + \epsilon p$ **if** $C(\theta) \geq 0$ **then** $p \leftarrow p - \epsilon \nabla_{\theta} U(\theta)$ **else** $r \leftarrow \frac{\nabla C(\theta)}{\|\nabla C(\theta)\|}$ $p \leftarrow p - 2(r'p)r$ **end if****end while** $\theta \leftarrow \theta + \epsilon p$ $p \leftarrow p - \frac{1}{2}\epsilon \nabla_{\theta} U(\theta)$

independent. To ensure that the HMC sampler lives within $C(\theta)$, we adopt the constrained HMC sampler from [Betancourt \(2011\)](#). A full description of the transition operation of the sampler is provided in [Algorithm S.1](#) where we write $\theta = \text{vech}(\theta)$ with a slight abuse of notation. Let $U(\theta)$ denote the negative of the logarithm of $\pi(\theta \mid \{\rho_{jk}\}_{j \leq k}, \mathbf{X})$ up to proportionality constants, i.e. $U(\theta) = -\sum_{i=1}^n \log q_{\theta}(X_{i\bullet}) + n \log z(\theta) - \sum_{j \leq k} \log \pi(\theta_{jk} \mid \rho_{jk})$, and $\nabla_{\theta} U(\theta)$ denote its gradient which is available following [Proposition 3.1](#) and due to the assumption that $\pi(\theta_{jk} \mid \rho_{jk})$ is differentiable. The new state generated according to [Algorithm S.1](#) is accepted with the standard Metropolis correction ([Neal et al., 2011](#), Section 5.3.2.1).

S.4 Additional Numerical Experiments

S.4.1 Likelihood vs. pseudo-likelihood based CIs in low dimensions

Results in Table S.1 substantiate that likelihood-based inference provides the best results in low-dimensions. For this, we generate data according to the same mechanism as in Section 7 of the main manuscript and consider $p = 3, 5$. We report the average coverage and width of 95% confidence intervals using bootstrap, over 100 replications. Results in Table S.1 indicate that while both maximum likelihood estimate (MLE) and pseudo maximum likelihood estimate (MPLE) have comparable coverage probabilities, widths of confidence intervals higher for PMLE, often by a factor as large as 10. No penalization was used in low dimensions, either for full likelihood or for pseudolikelihood.

			Ising				PGM			
Setting	p	n	Coverage		Width		Coverage		Width	
			MLE	MPLE	MLE	MPLE	MLE	MPLE	MLE	MPLE
LD	3	100	0.88 (0.08)	0.87 (0.07)	1.33 (0.38)	4.02 (2.86)	0.86 (0.35)	0.87 (0.34)	0.36 (0.16)	3.66 (3.88)
	5		0.80 (0.12)	0.82 (0.13)	1.34 (0.22)	4.98 (2.52)	0.66 (0.47)	0.67 (0.47)	0.37 (0.22)	4.17 (4.06)

Table S.1: Coverage and width of confidence intervals of maximum likelihood (MLE) and maximum pseudo-likelihood (MPLE) procedures for two PEGMs: Ising and PGM.

S.4.2 A comparison of RBM and BM representational power

Existing literature on training performance of the CD algorithm and its other versions focus mostly on benchmark datasets. Nonetheless, in this section we report the results of CD training versus the proposed approach in controlled simulation experiments. We compare the quality of the corresponding density estimate in terms of the total variation distance: $\text{TV}(p_{\theta_0}, p_{\hat{\theta}}) = \sum_{\mathbf{v} \in \{0,1\}^p} |p_{\theta_0}(\mathbf{v}) - p_{\hat{\theta}}(\mathbf{v})|$ where the dimension of θ_0 is the data generating value of the parameter and $\hat{\theta}$ is the estimate obtained from the two methods,

noting that the dimensions of θ_0 and $\hat{\theta}$ might be different given that the number of hidden variables is unknown in reality. We consider two cases $(p, m) = (2, 2)$ and $(p, m) = (3, 4)$ and set the sample size $n = 1000$. Elements of the true data generating θ_0 are set to 0 with probability 0.5 and are drawn from $\text{Uniform}[-1, 1]$ with probability 0.5, respecting the bipartite structure of the graph. When implementing CD we set $k = 1$, although we did not notice any significant difference in results for k up to 10. We report in Table S.2 results averaged over 50 replications where we abbreviate the proposed method here by FL (for *full likelihood*). All hyperparameters for training for the two algorithms are kept same, including the step size and convergence criteria. Two key observations can be made from the results. First, for increasing values of the number of hidden variables m , the fit is better, which is expected. Second, the performance of FL is better compared to CD in almost all cases, albeit by a small margin.

We next consider experiments where we study the representational power of RBMs to that of BMs. Since both method learn distributions of visible variables, we want to investigate whether allowing connections within layers as in BM (see also Figure 1), leads to similar or better learning power for a smaller number of hidden variables. For this we consider two situations $p = 3, 5$ which is the dimension of the visible variable. We generate the visible variables from a multivariate probit model where $y_j = \mathbb{I}(z_j > 0)$ and $z = (z_1, \dots, z_p)^T \sim \text{N}(0, \Sigma)$. We set $\Sigma = (\Sigma)_{ij}$ with $\Sigma_{ii} = 1$ and $\Sigma_{ij} = 0.5$, $i \neq j = 1, \dots, p$. This model is often used to capture dependent multivariate binary data (Ashford and Sowden, 1970; Chakraborty et al., 2023). We fix the sample size of the visible variables to $n = 1000$, and fit RBM and BM to the data letting the number of hidden variables m vary between 6–12 for $p = 3$, and 10–18 for $p = 5$, with increments of 1. Ideally, with enough hidden variables, RBMs should be able to approximate the data generating distribution (Le Roux and Bengio, 2008). We show the total variation distance between the true distribution and the fitted distribution from both models in Figure S.1, which

		$m = 4$	$m = 5$	$m = 6$
$p = 2$	FL	0.70	0.62	0.56
	CD	0.72	0.65	0.57
		$m = 16$	$m = 17$	$m = 18$
$p = 3$	FL	3.66	3.56	3.54
	CD	3.66	3.59	3.58

		m	RBM	BM
TV		20	60.29	48.91
		30	58.03	48.55
		40	55.38	46.09
		50	52.81	43.66

Table S.2: (*Left*) Training performance of RBMs using the proposed method (FL) and CD in terms of the estimated density of the visible variables with $p = 2, 3$ where we report the total variation distance between the true distribution and the estimated distribution. (*Right*) Results from a high-dimensional experiment (visible variable has dimension $p = 100$) where we report the total variation distance on a held-out test set. Throughout, m denotes the number of hidden variables.

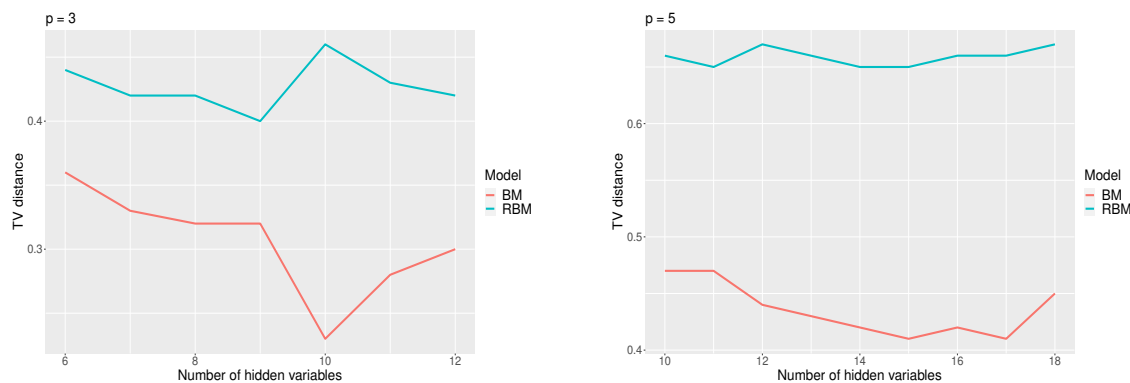


Figure S.1: RBM vs BM total variation distance when the dimension of the visible variables is $p = 3$ and 5.

reveals that BM achieves better approximation to the distribution of the visible variables with a fewer number of hidden variables, at least for this data generating distribution. Indeed, the gain in approximation for BM is almost 50% for $p = 3$ and 33% for $p = 5$. The trade-off is the computation time. The key bottleneck of training a full BM is the fact that the conditional distribution of the hidden variables depend on the corresponding visible variables which is not the case for RBMs. This allows for much faster training of RBMs. While a theoretical investigation into the representational power of BM is beyond the scope of this work, we hope that our numerical experiments serve as a platform for further investigation into the properties of a full BM.

Next, we report our results from a high-dimensional experiment comparing the representational power of RBM and BM with different choices of the number of hidden variables. Here, we consider $p = 100$, and let $m = 20, 30, 40, 50$. The observed data is generated from a probit model as before. Estimating the total-variation distance for this very large sample space is computationally prohibitive. Instead, we compare the fit on a test set of size $n_t = 500$. Specifically, we compute $\sum_{\mathbf{v} \in \mathcal{T}} |p(\mathbf{v}) - p_{\hat{\theta}}(\mathbf{v})| = \text{TV}$, where \mathcal{T} is the set of test points and $p_{\hat{\theta}}(\mathbf{v})$ is computed following Remark 5.3 in the main document. We randomly selected 50 configurations of the hidden variables from $\{0, 1\}^m$. Using each of these configurations, we obtained an estimate of $p_{\hat{\theta}}(\mathbf{v})$ for $\mathbf{v} \in \mathcal{T}$. A final estimate is constructed using the average of these estimates, which is then used to compute TV as defined above. In the right panel of Table S.2 we report the results, which reconfirms that for the same number of hidden variables, the representational power of BM seems to be better than that of an RBM.

S.5 Additional Data Analysis Results

S.5.1 Additional results for movie ratings network

This section presents additional results from fitting the Ising model to the *Movielens* dataset using the PMLE-based method described as in Section 8.1. Our primary focus is to reveal the connections among the most frequently rated 50 movies. The resulting graph structure is shown in Figure S.2, left panel. Table S.3 provides the match between abbreviations and the legends of the movie titles, genres, and years of release. We also present the top 13 most connected movies from the resulting graph structure in Table S.4. The top three of them are from two well known movie franchises. These two movie franchises (*Star Wars* and *Lord of the Rings*) also form two separate cliques within the graph, as shown in Figure S.2, right panel. A heatmap of estimated $\hat{\theta}_{\lambda}$ with the penalty parameter $\lambda = 10$ is

in Figure S.3, where red and blue denote positive and negative connections.

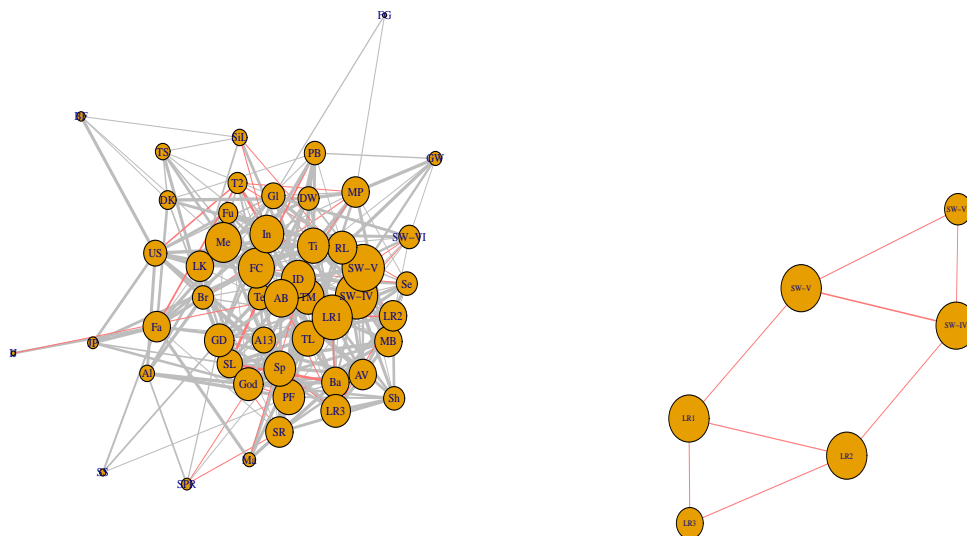


Figure S.2: (*Left*). The movie ratings network from the PMLE-based Ising model. The edge widths are proportional to the stable selection probability, and the node sizes are proportional to the degree. Red and gray denote positive and negative edges. (*Right*). Extracted subgraph of the movie ratings network with *Star Wars* and *Lord of the Rings* franchises.

Abbr.	Title (Year)	Genres
TS	Toy Story (1995)	Adventure Animation Children Comedy Fantasy
Br	Braveheart (1995)	Action Drama War
MP	Monty Python and the Holy Grail (1975)	Adventure Comedy Fantasy
SW-V	Star Wars: Episode V - The Empire Strikes Back (1980)	Action Adventure Sci-Fi
PB	Princess Bride (1987)	Action Adventure Comedy Fantasy Romance
RL	Raiders of the Lost Ark (1981)	Action Adventure
SW-VI	Star Wars: Episode VI - Return of the Jedi (1983)	Action Adventure Sci-Fi
Te	Terminator(1984)	Action Sci-Fi Thriller
GD	Groundhog Day (1993)	Comedy Fantasy Romance
BF	Back to the Future (1985)	Adventure Comedy Sci-Fi
IJ	Indiana Jones and the Last Crusade (1989)	Action Adventure
A13	Apollo 13 (1995)	Adventure Drama IMAX
MB	Men in Black (1997)	Action Comedy Sci-Fi
GW	Good Will Hunting (1997)	Drama Romance
Ti	Titanic (1997)	Drama Romance
SPR	Saving Private Ryan (1998)	Action Drama War
Ma	Matrix (1999)	Action Sci-Fi Thriller
SW-IV	Star Wars: Episode IV - A New Hope (1977)	Action Adventure Sci-Fi
SS	Sixth Sense (1999)	Drama Horror Mystery
AB	American Beauty (1999)	Drama Romance
FC	Fight Club (1999)	Action Crime Drama Thriller
PF	Pulp Fiction (1994)	Comedy Crime Drama Thriller
SR	Shawshank Redemption (1994)	Crime Drama
TM	Twelve Monkeys (1995)	Mystery Sci-Fi Thriller
AV	Ace Ventura: Pet Detective (1994)	Comedy
FG	Forrest Gump (1994)	Comedy Drama Romance War
Gl	Gladiator (2000)	Action Adventure Drama
LK	Lion King (1994)	Adventure Animation Children Drama Musical IMAX
Sp	Speed (1994)	Action Romance Thriller
TL	True Lies (1994)	Action Adventure Comedy Romance Thriller
Me	Memento (2000)	Mystery Thriller
Sh	Shrek (2001)	Adventure Animation Children Comedy Fantasy Romance
Fu	Fugitive (1993)	Thriller
Se	Seven (1995)	Mystery Thriller
JP	Jurassic Park (1993)	Action Adventure Sci-Fi Thriller
LR1	Lord of the Rings: The Fellowship of the Ring (2001)	Adventure Fantasy
US	Usual Suspects, The (1995)	Crime Mystery Thriller
SL	Schindler's List (1993)	Drama War
DK	Dark Knight (2008)	Action Crime Drama IMAX
Al	Aladdin (1992)	Adventure Animation Children Comedy Musical
T2	Terminator 2: Judgment Day (1991)	Action Sci-Fi
DW	Dances with Wolves (1990)	Adventure Drama Western
Ba	Batman (1989)	Action Crime Thriller
SiL	Silence of the Lambs (1991)	Crime Horror Thriller
LR2	Lord of the Rings: The Two Towers (2002)	Adventure Fantasy
Fa	Fargo (1996)	Comedy Crime Drama Thriller
LR3	Lord of the Rings: The Return of the King (2003)	Action Adventure Drama Fantasy
ID	Independence Day (1996)	Action Adventure Sci-Fi Thriller
In	Inception (2010)	Action Crime Drama Mystery Sci-Fi Thriller IMAX
God	Godfather (1972)	Crime Drama

Table S.3: Abbreviations for the movie data set.

Title (Year)	Number of Degree
Star Wars: Episode IV - A New Hope (1977)	20
Star Wars: Episode V - The Empire Strikes Back (1980)	20
Lord of the Rings: The Fellowship of the Ring (2001)	19
Fight Club (1999)	17
Memento (2000)	17
Independence Day (1996)	16
American Beauty (1999)	16
Inception (2010)	16
Twelve Monkeys (1995)	15
Pulp Fiction (1994)	15
Speed (1994)	15
True Lies (1994)	15
Titanic (1997)	15

Table S.4: Movies with the highest degree of connectivity: top 13.

Estimated Theta for the Movie Ratings Network via MLE-based Ising Model

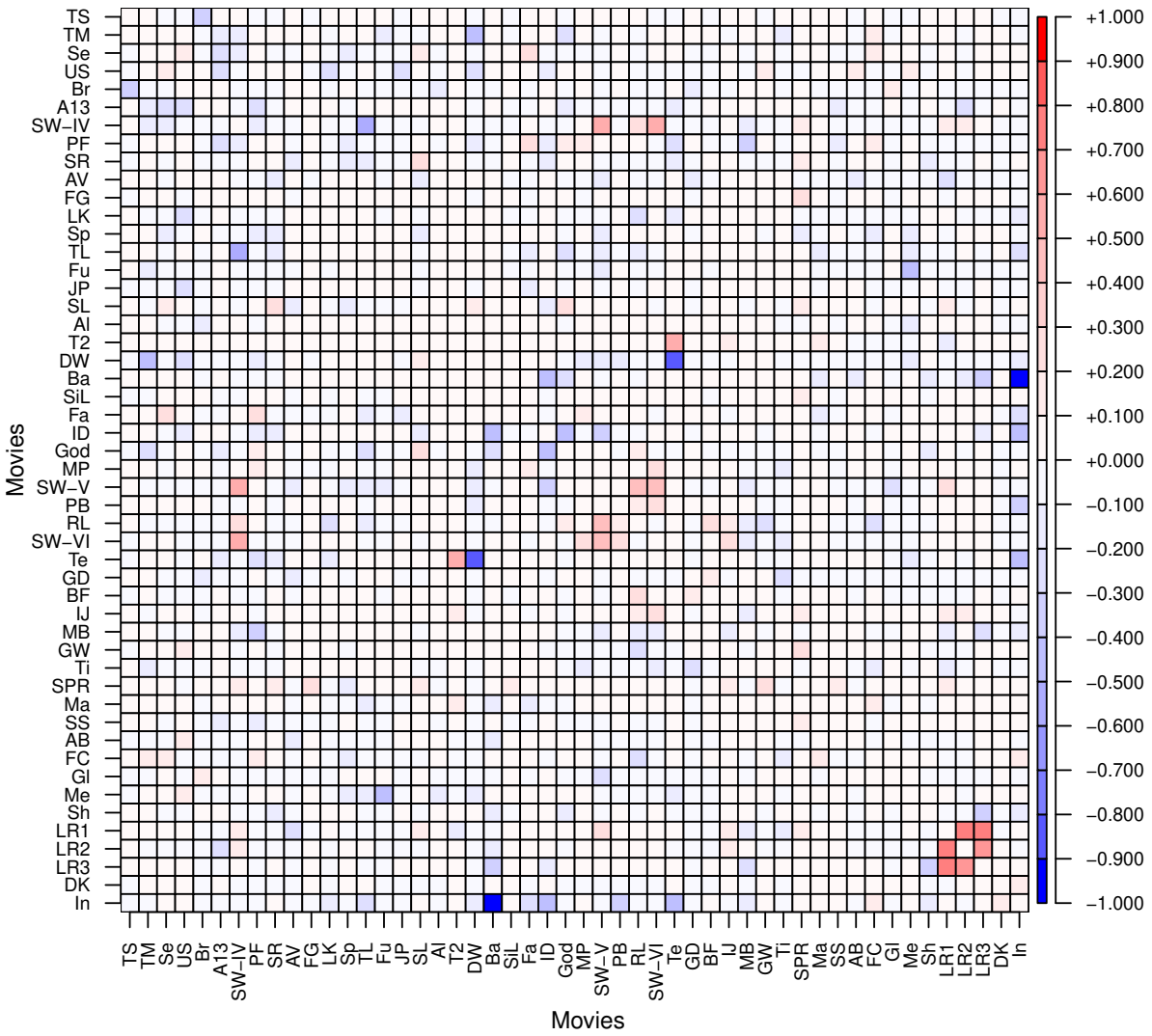


Figure S.3: Parameter estimates for the movie ratings network.

S.5.2 Additional results for breast cancer network

Additional results on the breast cancer miRNA networks from the full-likelihood fit and pseudo-likelihood fit of PGM discussed in Section 8.3 are presented below. The dependency structures among miRNA expression profiles of 353 genes modeled by the aforementioned methods are comparable, as shown in Figures S.4 and S.5. These two figures contain subgraphs of the resulting networks of the two methods. Common edges in from the two networks are colored blue.

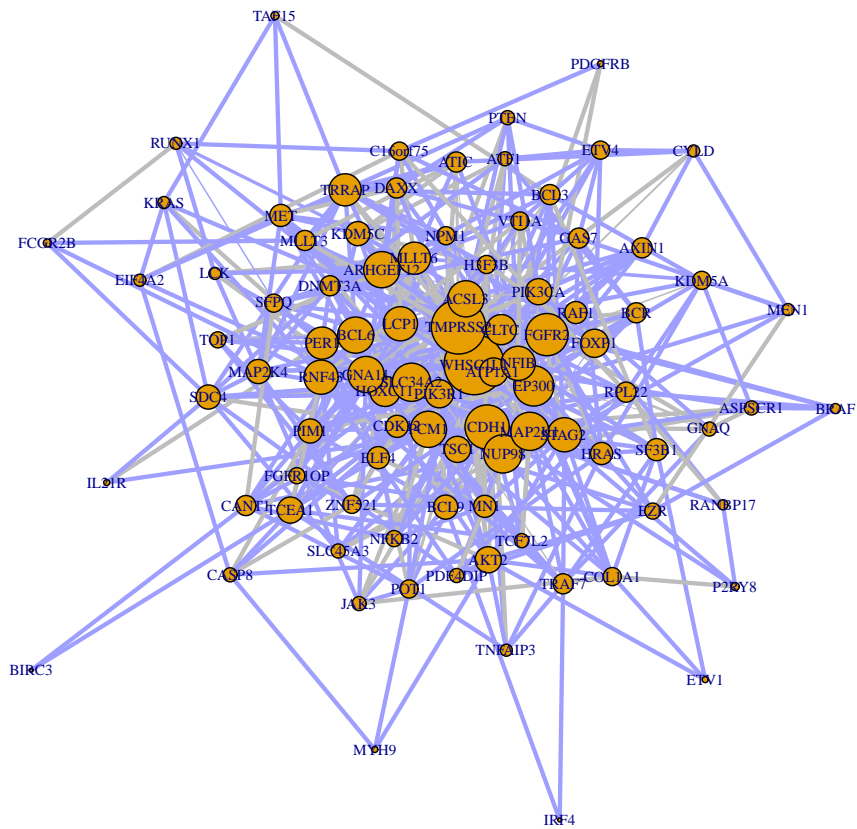


Figure S.4: Subgraph of a PGM network for the Breast Cancer miRNA Network obtained using the full-likelihood method. Nodes with degrees of at least 5 in the full network are plotted here. The edge widths are proportional to the stable selection probability, and the node sizes are proportional to the degree. Blue edges appear in both full-likelihood and pseudo-likelihood networks.

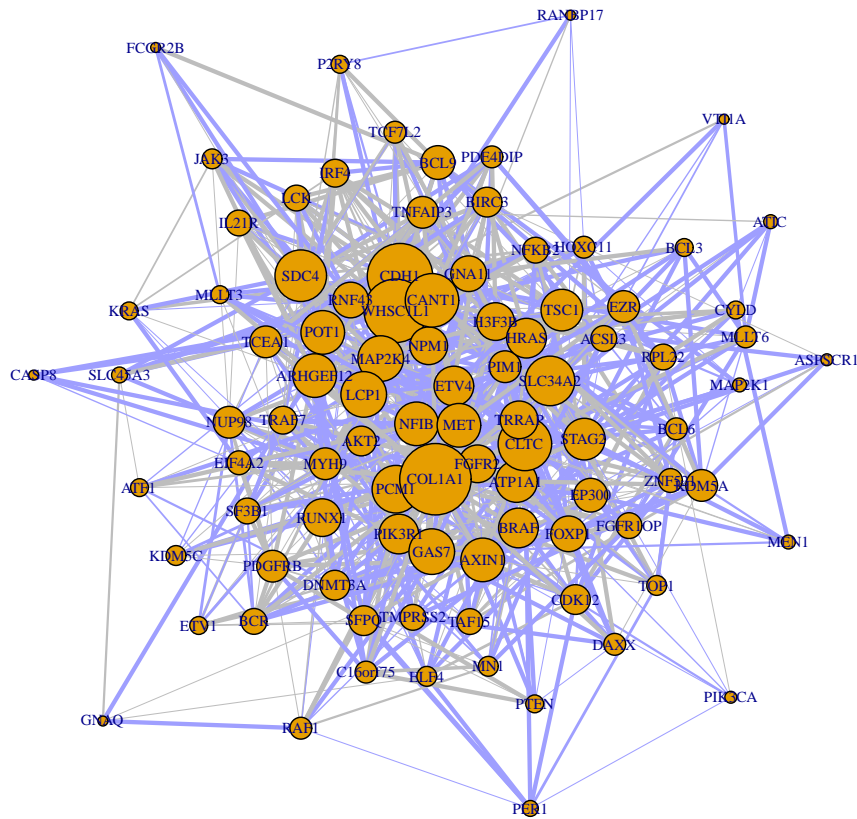


Figure S.5: Subgraph of a PGM network for the Breast Cancer miRNA Network obtained using the pseudo-likelihood method. Nodes with degrees of at least 5 in the full network are plotted here. The edge widths are proportional to the stable selection probability, and the node sizes are proportional to the degree. Blue edges appear in both full-likelihood and pseudo-likelihood networks.